Millennial slip rate of the Longitudinal Valley fault from river terraces : implications for convergence across the active suture of eastern Taiwan

Shyu, J. Bruce H.; Sieh, Kerry; Avouac, Jean-Philippe; Chen, Wen-Shan; Chen, Yue-Gau

2006

https://hdl.handle.net/10356/95555

https://doi.org/10.1029/2005JB003971

Millennial slip rate of the Longitudinal Valley fault from river terraces: Implications for convergence across the active suture of eastern Taiwan

J. Bruce H. Shyu,[1] Kerry Sieh,[1] Jean-Philippe Avouac,[1] Wen-Shan Chen,[2] and Yue-Gau Chen[2]

[1] The Longitudinal Valley fault is a key element in the active tectonics of Taiwan. It is the principal structure accommodating convergence across one of the two active sutures of the Taiwan orogeny. To understand more precisely its role in the suturing process, we analyzed fluvial terraces along the Hsiukuluan River, which cuts across the Coastal Range in eastern Taiwan in the fault's hanging wall block. This allowed us to determine both its subsurface geometry and its long-term slip rate. The uplift pattern of the terraces is consistent with a fault-bend fold model. Our analysis yields a listric geometry, with dips decreasing downdip from about 50° to about 30° in the shallowest 2.5 km. The Holocene rate of dip slip of the fault is about 22.7 mm/yr. This rate is less than the 40 mm/yr rate of shortening across the Longitudinal Valley derived from GPS measurements. The discrepancy may reflect an actual difference in millennial and decadal rates of convergence. An alternative explanation is that the discrepancy is accommodated by a combination of slip on the Central Range fault and subsidence of the Longitudinal Valley floor. The shallow, listric geometry of the Longitudinal Valley fault at the Hsiukuluan River valley differs markedly from the deep listric geometry illuminated by earthquake hypocenters near Chihshang, 45 km to the south. We hypothesize that this fundamental along-strike difference in geometry of the fault is a manifestation of the northward maturation of the suturing of the Luzon volcanic arc to the Central Range continental sliver.

1. Introduction

[2] The Taiwan orogen is the product of ongoing collision between the Eurasian and Philippine Sea plates [e.g., *Ho*, 1986; *Teng*, 1987, 1990, 1996, and references therein] (Figure 1). This collision, which started a few million years ago, has created two belts of active structures on and around the island [*Malavieille et al.*, 2002; *Shyu et al.*, 2005a]. Frequent ruptures of these active faults have made Taiwan one of the most seismically active places on Earth [e.g., *Bonilla*, 1975, 1977; *Hsu*, 1980; *Cheng and Yeh*, 1989]. The most notable recent earthquake, the disastrous Chi-Chi earthquake of 1999, was produced by rupture of the Chelungpu fault, one of the many major active faults constituting Taiwan's western neotectonic belt [e.g., *Chen et al.*, 2001; *Kelson et al.*, 2001].

[3] Along the eastern flank of the island, the linear, north-south trending Longitudinal Valley, which separates the Central and Coastal Ranges, marks the suture between an accreted volcanic island arc and a continental sliver. The Longitudinal Valley fault, one of the most active structures on the island, dominates this eastern neotectonic belt [e.g., *Angelier et al.*, 1997; *Shyu et al.*, 2005a] (Figure 2). This east dipping left-lateral reverse fault accommodates rapid uplift of the Coastal Range on its hanging wall block [e.g., *Yu and Liu*, 1989; *Hsu et al.*, 2003]. Several large seismic ruptures of this fault have occurred in the past century [*Hsu*, 1962; *Bonilla*, 1975, 1977; *Cheng et al.*, 1996]. Part of the fault is also creeping aseismically at rates up to 20 mm/yr [e.g., *Angelier et al.*, 1997; *Lee et al.*, 2001, 2003]. Hypocenters of small earthquakes illuminate the fault plane and show that it has a listric geometry near the town of Chihshang [*Chen and Rau*, 2002; *Kuochen et al.*, 2004]. Elsewhere, however, the geometry of the fault remains poorly known.

[4] According to GPS results, about 30−40 mm/yr of oblique convergence is currently taken up between the Central Range block and the Coastal Range block [e.g., *Yu et al.*, 1997; *Hsu et al.*, 2003] (Figure 3). Whereas most

---

[1]Tectonics Observatory, Division of Geological and Planetary Sciences, California Institute of Technology, Pasadena, California, USA.
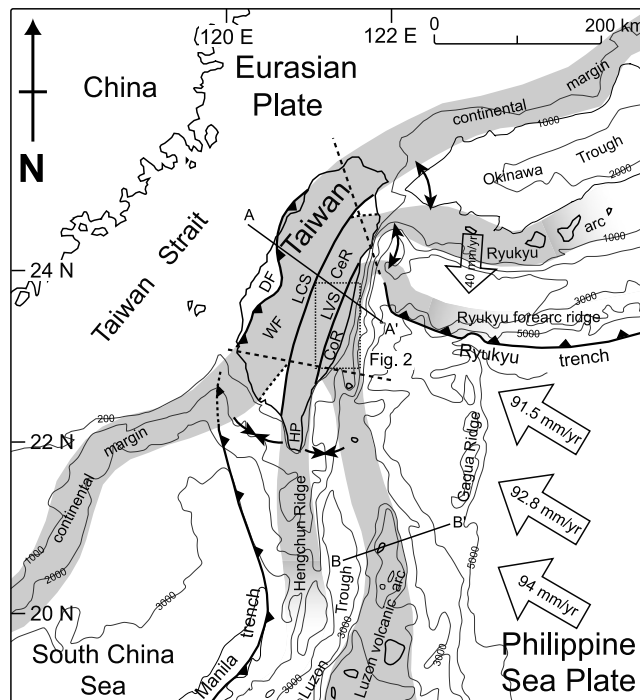[2]Department of Geosciences, National Taiwan University, Taipei, Taiwan.

Figure 1. Taiwan orogen being created by a tandem suturing of the Luzon volcanic arc and a sliver of continental crust to the Chinese continental margin. The Longitudinal Valley suture (LVS), in eastern Taiwan, represents the eastern of the two sutures, joining the Coastal Range (CoR) and the Central Range (CeR) blocks. Current velocity vectors of the Philippine Sea plate relative to south China, at 124°E and 20°, 21°, and 22°N, are calculated using the Recent plate velocity model (REVEL) of *Sella et al.* [2002]. Current velocity vector of the Ryukyu arc is adapted from *Lallemand and Liu* [1998]. Black dashed lines are the northern and western limits of the Wadati-Benioff zone of the two subduction zones, taken from the seismicity database of the Central Weather Bureau, Taiwan. DF, deformation front; LCS, Lishan-Chaochou suture; WF, Western Foothills; HP, Hengchun Peninsula. Adapted from *Shyu et al.* [2005b] with permission from Elsevier.

of this convergence may be absorbed by left-lateral reverse slip along the Longitudinal Valley fault, the Coastal Range, in the hanging wall block of the fault, is not a large mountain range: Its maximum elevation is only about 1.6 km, significantly lower than the 4-km-high peaks of the Central Range. Therefore one may suspect that other mechanisms, such as possible underthrusting of the Longitudinal Valley floor, may accommodate at least some of the plate convergence, or that the Longitudinal Valley fault is a relatively young feature of the Taiwan orogen.

[5] Better knowledge of the slip rates, geometry and history of the Longitudinal Valley fault, as well as its relationship to other structures, is important both in quantifying the seismic hazard of eastern Taiwan and in the understanding the tectonic kinematics and evolution of the island. More broadly, these pursuits would enhance our knowledge of the general processes of arc-arc or arc-continent collisions.

[6] Near the middle of the Longitudinal Valley, the Hsiukuluan River cuts through the Coastal Range and flows eastward to the Philippine Sea. Along this segment of the river (hereafter referred to as Hsiukuluan canyon) are many levels of fluvial terraces [e.g., *Chang et al.*, 1992] (Figure 4), which provide a record of fluvial incision. Since the Hsiukuluan River is the only river that flows through the Coastal Range, these fluvial terraces provide a unique opportunity to assess long-term patterns and rates of uplift
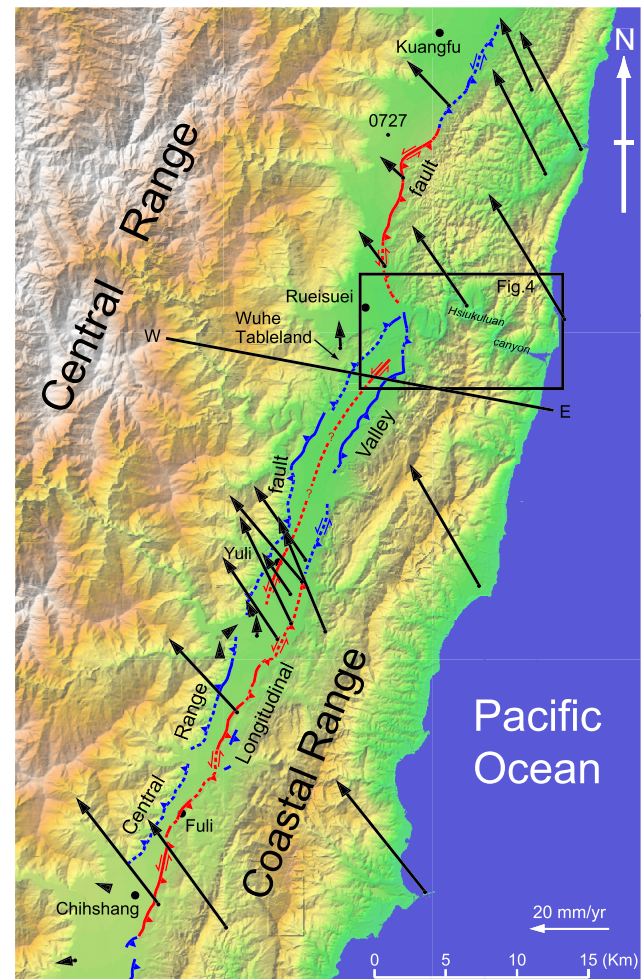
Figure 2. Map of major structures in the middle part of the Longitudinal Valley. The Longitudinal Valley fault is an east dipping, obliquely slipping reverse fault, along which the Coastal Range is rising rapidly and moving toward the Central Range. The less prominent Central Range fault is a west dipping reverse fault, above which many fluvial terraces and the Wuhe Tableland are rising slowly. Faults that ruptured during the 1951 earthquakes are red. Major faults and flexures that did not rupture in 1951 but are known to be active are blue. Adapted from *Shyu et al.* [2006a]. Black arrows are GPS vectors for the period 1993 to 1999 [*Hsu et al.*, 2003]. Motions are relative to station 0727, about 7 km southwest of Kuangfu. The differences between vectors indicate shortening across the valley of about 40 mm/yr.

of the range. The uplift rates, when used in conjunction with information about bedding dips of Coastal Range bedrock, can then be used to constrain the geometry and dip-slip rate for the Longitudinal Valley fault.

[7] In this paper, we first review the geologic setting of the Coastal Range and the Longitudinal Valley. We then describe the characteristics of the fluvial terraces along Hsiukuluan canyon, especially along the western half of the river valley, where the terraces are more prominent. Age

determinations of various terrace levels allow us to calculate incision rates along the river, which we can relate to uplift rates of the Coastal Range. These uplift rates and their spatial relationships provide information about the geometry and long-term dip-slip rate of the Longitudinal Valley fault.

2. General Geologic Setting

[8] Taiwan is at the boundary of the Philippine Sea plate and the South China block of the Eurasian plate. South of
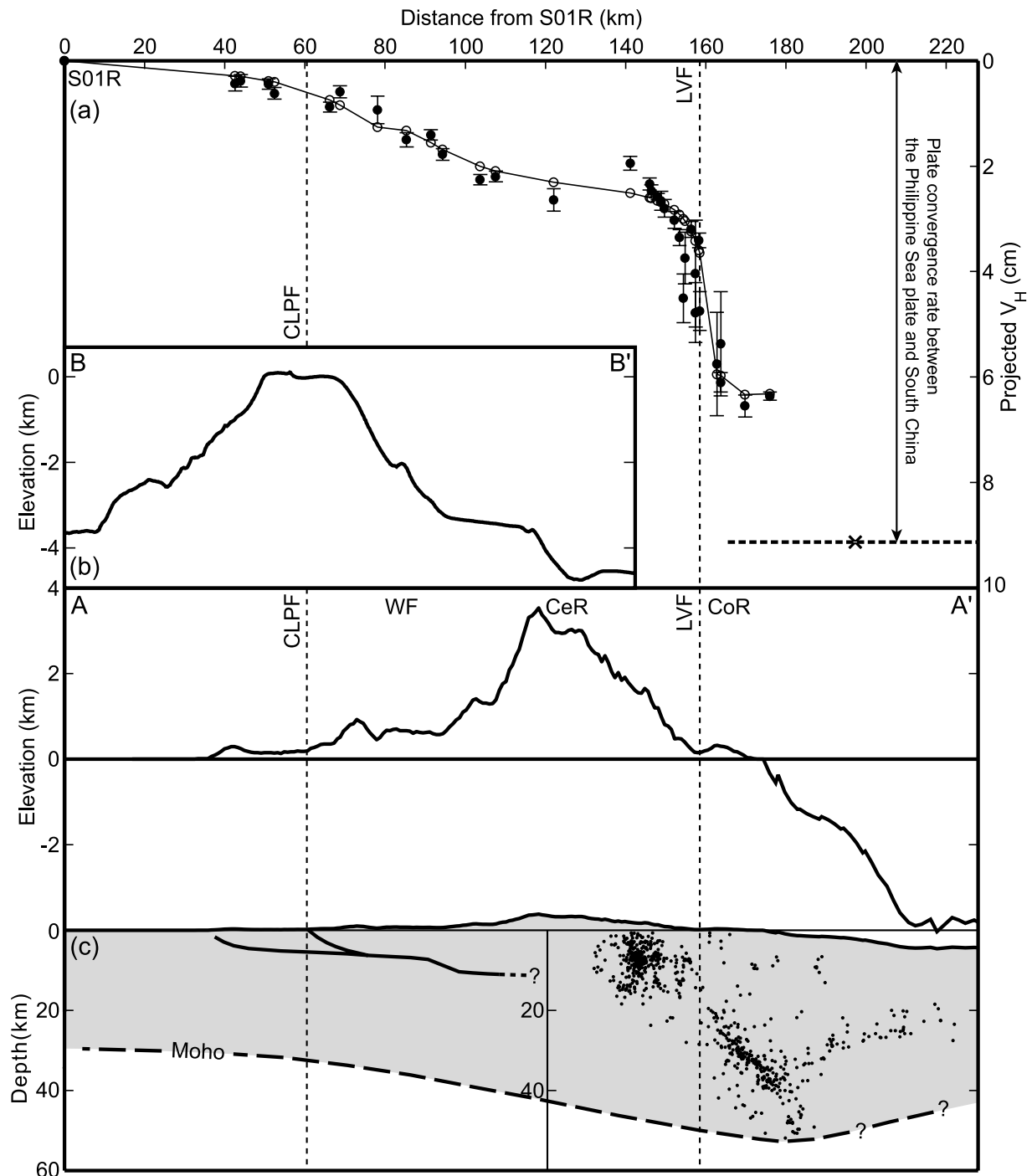

Figure 3

Taiwan, the 90 mm/yr convergence between these two blocks (Figure 1) is absorbed by subduction of the South China Sea along the Manila trench. At the latitude of Taiwan, the continental margin of the South China Sea has impinged upon the trench, so the convergence is absorbed by deformation of the continental margin, which has resulted in the formation of the mountainous island of Taiwan.

[9] The Taiwan orogen is the product of a tandem suturing and tandem disengagement of the Asian continental margin, the Luzon volcanic island arc, and a thin intervening continental sliver [*Shyu et al.*, 2005b] (Figure 1). In the south, the three lithospheric blocks have begun colliding. Both collisions mature northward, creating the main body of the island and the numerous active thrust faults and folds that are manifestations of the double suturing. A tandem disengagement occurs in the northeastern quarter of the island above the Ryukyu subduction zone, where normal faulting is dominant and the three lithospheric blocks are separating along the two sutures. The Central Range, Taiwan's mountainous backbone, is the exhumed portion of a sliver of continental lithosphere, flanked on the east by the Coastal Range, the attached part of the Luzon volcanic arc. Between these two linear mountain ranges is the Longitudinal Valley, the locus of the suture between the continental sliver and the collided volcanic arc.

[10] Two major structures dominate the Longitudinal Valley. On the eastern side of the valley, the east dipping Longitudinal Valley fault has long been considered one of the most important and active faults in Taiwan [e.g., *Angelier et al.*, 1997; *Shyu et al.*, 2005a]. It is characterized by high rates of sinistral reverse motion. Near the town of Chihshang (Figure 2), this fault is creeping aseismically at a high rate [e.g., *Angelier et al.*, 1997]. A creepmeter measurement reveals a one-dimensional shortening rate of about 20 mm/yr [*Lee et al.*, 2001, 2003]. Geodetic measurements suggest that the rates of sinistral motion of the fault are similar to that of reverse motion [e.g., *Yu et al.*, 1992, 1997]. The most recent surface rupture occurred along the Longitudinal Valley fault during an earthquake couplet in 1951 [*Shyu et al.*, 2006a]. This seismic rupture extended into the rapid creeping segment. Thus the Chihshang segment of the Longitudinal Valley fault exhibits both aseismic and seismic

strain relief and its long-term slip rate is likely to be higher than the 20 mm/yr measured by creepmeter.

[11] The other major fault of the Longitudinal Valley is the Central Range fault, which crops out along the western flank of the valley [*Biq*, 1965; *Shyu et al.*, 2005a, 2006b]. This fault is a west dipping thrust fault, above which the eastern flank of the Central Range is rising above the valley.

[12] The Coastal Range is the shortened and accreted part of the Luzon volcanic arc and its forearc basin [e.g., *Huang et al.*, 1997; *Chang et al.*, 2001]. It is composed of an assemblage of young (Miocene through early Pliocene) volcanic arc rocks and associated turbidite deposits, mélange, and fringing-reef limestones [e.g., *W.-S. Chen*, 1988; *Ho*, 1988] (Figure 5). The major geologic unit of the range is the Tuluanshan Formation, mostly andesitic volcanic sediments, such as breccias and tuffs. It forms the highest peaks and ridges of the range. Bordering the volcanic sediments are deep-marine turbidites, including the Fanshuliao and Paliwan formations [*Teng*, 1980; *Teng et al.*, 1988]. The latter has abundant metamorphic rock fragments derived from the Central Range, which indicate the exposure and proximity of the Central Range during its deposition in a forearc basin [*Teng*, 1982]. In the southern part of the Coastal Range, the Lichi Formation, with its highly sheared clays and severely fragmented sedimentary sequences, is likely to be a highly shortened section of the forearc basin. Pieces of mafic and ultramafic rocks within the Lichi Formation may be remnants of the forearc oceanic crust [e.g., *Chang et al.*, 2001].

[13] In the middle part of the Coastal Range, the Chimei fault forms a major bedrock boundary between the volcanic Tuluanshan Formation and the sedimentary Paliwan Formation (Figures 4 and 5). Since the deep marine Paliwan Formation was deposited at a water depth of several thousand meters, more than a thousand meters of reverse movement along the Chimei fault created the current juxtaposition of the two formations [e.g., *Chen et al.*, 1991].

3. River Terraces of Hsiukuluan Canyon
3.1. Distribution and Characteristics
[14] The Hsiukuluan River is the largest river in the Longitudinal Valley. Most of its larger tributaries drain the

Figure 3. (a) A GPS transect across the Taiwan orogen (adapted from *Hsu et al.* [2003] with permission from Elsevier). The transect trends 306° and includes measurements within a swath about 60 km wide, approximately along line A-A′ in Figure 1. About 40 mm/yr of horizontal shortening is currently absorbed across this section of the Longitudinal Valley. The western Taiwan neotectonic belt, which includes the Chelungpu fault (CLPF), absorbs the remaining ∼20 mm/yr of horizontal shortening. Solid points are the observed velocities along 306°, and circles are the predicted points using a two-dimensional interseismic dislocation model. All points are relative to station S01R in the Penghu Islands, which can be considered to be on the stable south China continental block [e.g., *Sella et al.*, 2002]. The plate convergence rate between the Philippine Sea plate and south China, calculated using the Recent plate velocity model (REVEL) of *Sella et al.* [2002], is also along 306° and about 20 mm/yr greater than the convergence rate across the transect. LVF, Longitudinal Valley fault. (b) Topographic profiles across Taiwan along line A-A′ and, for comparison, across an undeformed volcanic island of the Luzon arc along line B-B′ in Figure 1. Vertical exaggeration is 10 times. WF, Western Foothills; CeR, Central Range; CoR, Coastal Range. (c) Several major crustal structural features along the A-A′ profile across Taiwan. A shorter profile of seismicity across eastern Taiwan, at the same location but with about half the width, shows two notable planes of seismicity [*Kuochen et al.*, 2004]. A simplified structural cross section of the Western Foothills shows a décollement at a depth of about 6–10 km (modified from *Yue et al.* [2005]). The depth of Moho across Taiwan, compiled from *Kim et al.* [2004], *Lin* [2005], and *McIntosh et al.* [2005], appears to be deepest beneath the Coastal Range, at about 50 km, and shallows to the west. No vertical exaggeration.
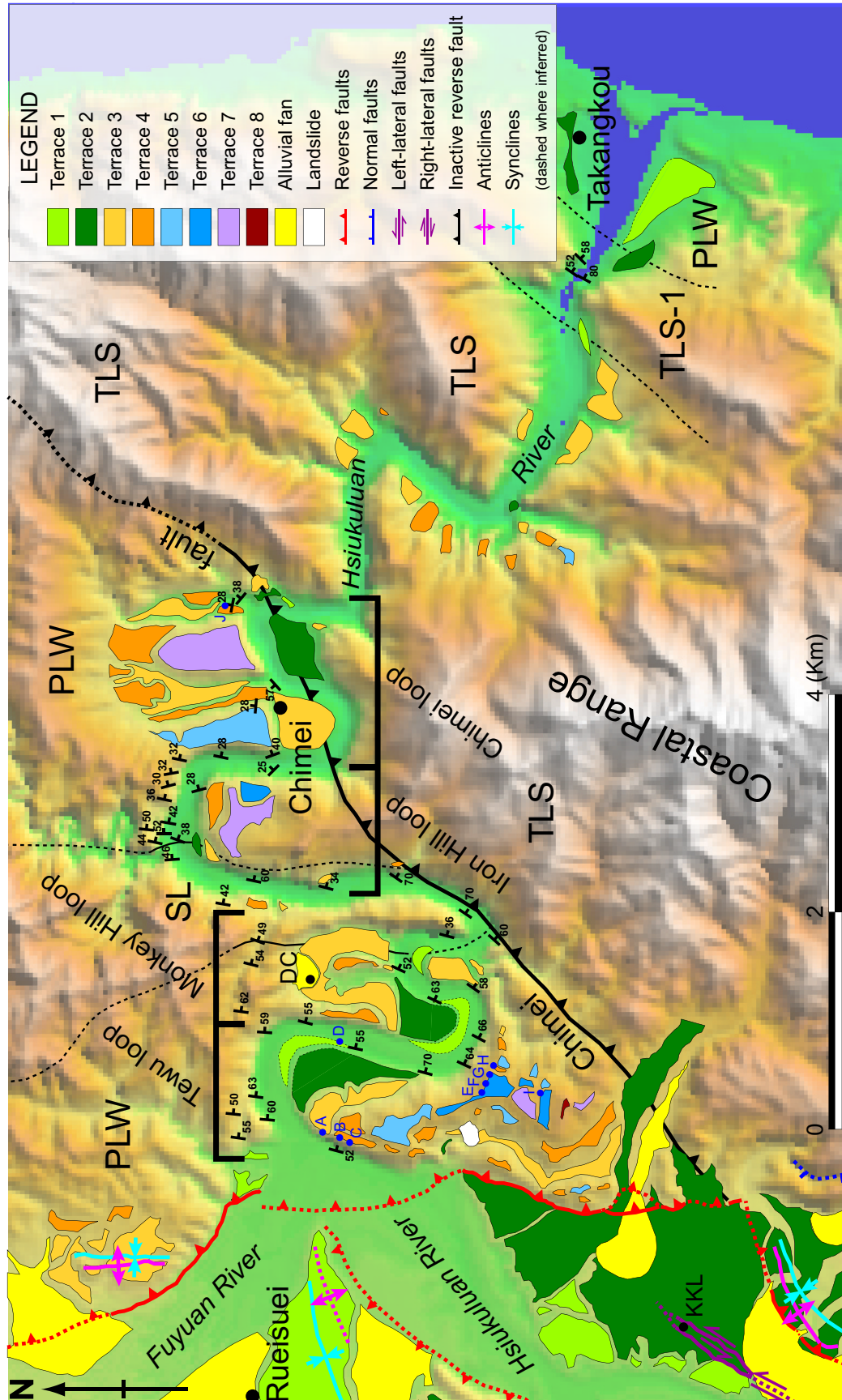
Figure 4. Hsiukuluan River across the Coastal Range. Since the Hsiukuluan River is the only river that flows across the Coastal Range, it provides a unique opportunity to determine the long-term rates of uplift of the range. Along the western part of its course across the range, the river has formed the deeply incised Tewu, Monkey Hill, Iron Hill, and Chimei meander loops. As many as eight levels of fluvial terraces exist on both sides of the river valley. PLW, sedimentary Paliwan Formation; SL, Shuilien Conglomerate Member of the Paliwan Formation; TLS, volcanic rocks of the Tuluanshan Formation; TLS-1, a thick layer of volcanic breccia within the Tuluanshan Formation. Dark blue dots indicate where the thickness of the fluvial terrace deposit was directly measured.

Figure 5. A schematic geologic cross section across the Longitudinal Valley near Hsiukuluan canyon showing the princip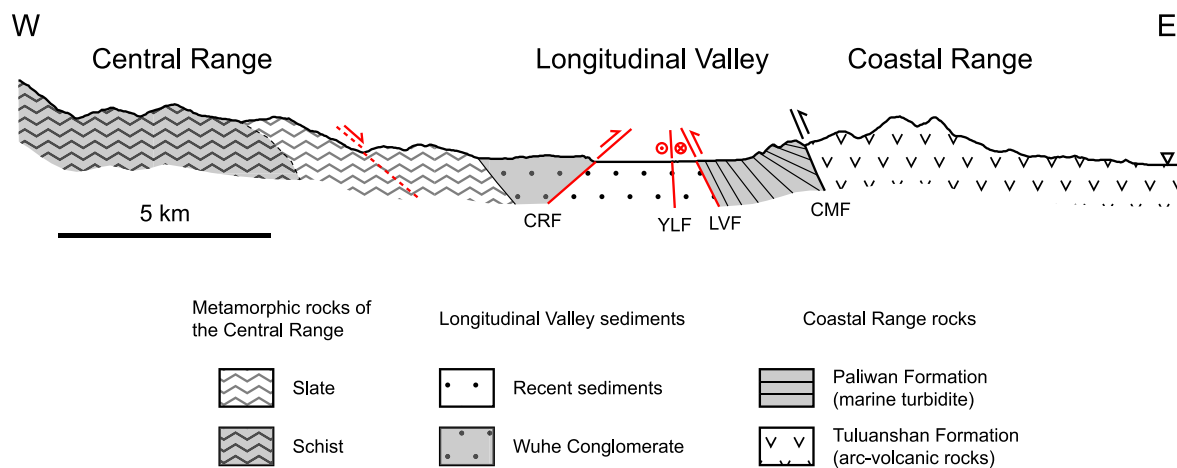al active structures of the suture and major rock units in the vicinity. The location of the cross section is shown in Figure 2. The Coastal Range consists of the arc-volcanic Tuluanshan Formation and the marine turbidite of the Paliwan Formation. The Central Range, in the west, is composed of metamorphosed slates and schists. Between the east dipping Longitudinal Valley fault (LVF) and the west dipping Central Range fault (CRF) are fluvial sediments of the valley. One objective of this paper is to determine how convergence across the Longitudinal Valley suture is partitioned between these two faults. CMF, Chimei fault; YLF, Yuli fault.

eastern flank of the Central Range south of Rueisuei, but several smaller ones drain the western flank of the Coastal Range. East of Rueisuei, the Hsiukuluan River is joined by the Fuyuan River, its only tributary north of Rueisuei. At this juncture the river turns 90° to the east and enters the Coastal Range (Figure 4). Between the confluence and the village of Chimei, approximately 4 km downstream, the river flows in deeply incised meanders, characterized by many levels of strath terraces, commonly sequestered in older, abandoned meander loops.

[15] Four major meander loops exist in Hsiukuluan canyon. We call these the Tewu, Monkey Hill, Iron Hill and Chimei loops, after local village names (Figure 4). Only the Tewu and Iron Hill meanders are active today. Most of the Monkey Hill and Chimei loops are abandoned.

[16] The Tewu loop is the farthest upstream, constituting the first reach of the river as it flows into the Coastal Range. Eight preserved terrace levels rise above the modern riverbed on the inside, southern bank of the meander loop (Figure 4). Since the horizontal distance from the highest terrace to the modern riverbed is much greater than the vertical separation of the two, northward lateral migration is clearly occurring at a higher rate than incision [Hovius and Stark, 2001].

[17] Multiple terrace levels are also present within the Chimei loop, along the northern bank of the modern river (Figure 4). A large abandoned meander channel is present immediately downstream of the village of Chimei. Including the abandoned channel, there are five terrace levels above the modern riverbed.

[18] Fewer terrace levels are present within the Monkey Hill and Iron Hill loops. At Monkey Hill, the major terrace is the abandoned meander channel (terrace 3 in Figure 4). About four levels of terraces are present at the Iron Hill loop. Two of them, however, are quite small.

[19] In fluvial geomorphology, terraces are generally divided into two types: Strath terraces are those underlain by no more than a few meters of fluvial sediment atop a bedrock erosional surface, or strath; alluvial (or fill) terraces sit atop tens or even hundreds of meters of fluvial sediment [e.g., Bull, 1990; Bull and Knuepfer, 1987]. The formation of strath terraces generally indicates rock uplift, but most alluvial terraces document aggradation and incision of rivers associated with other hydrological processes, such as base level change and change in sediment supply, both commonly associated with climatic fluctuations [e.g., Bull, 1990; Bull and Knuepfer, 1987].

[20] Although alluvial terraces are common in Taiwan [e.g., Hsieh et al., 1994; Liew and Hsieh, 2000], Hsiukuluan canyon is dominated by strath terraces (Figure 6). For example, numerous outcrops within the Tewu loop reveal sediment thicknesses of less than 10 m above the terrace straths (Table 1). Only the abandoned meander loop near Monkey Hill may have thicker sediment cover. A drill core on that terrace (DC in Figure 4) reveals 28 m of sediment above the terrace strath [Hsieh et al., 2003]. However, since the location of the core is on a small alluvial fan, some of this must be fan sediment deposited after abandonment of the paleochannel.

[21] A layer of fine-grained overbank sediment caps the fluvial gravels of all river terrace sequences (Figure 6). The thickness of this fine-grained layer appears to be greater on the older terraces, but thicknesses commonly range between 2 and 4 m. On some of the Tewu terraces, a fining upward sequence above the fluvial gravels is consistent with a point bar origin.

[22] Several meters of gravel underlie the overbank deposits (Figure 6). Except for the highest three terraces of the Tewu loop, all of the gravel layers consist predominantly of subrounded metamorphic clasts derived from the
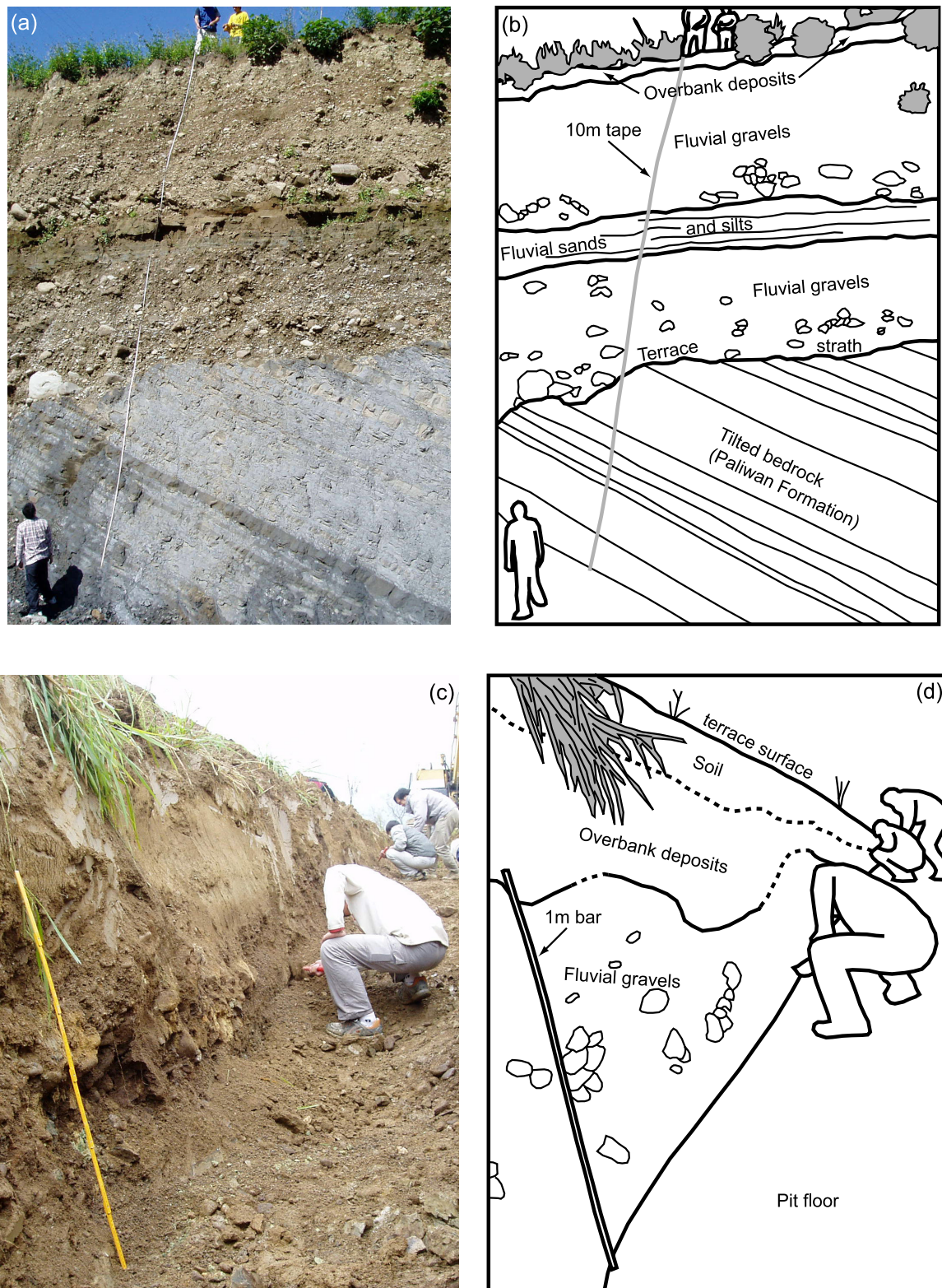
Figure 6. Typical exposures of the river terrace deposits along the western Hsiukuluan canyon. (a) Photograph and (b) sketch of an outcrop at site CYC (terrace 4). Typical terrace sediments include several meters of fluvial sands and gravels overlying the bedrock strath. The length of the white tape is 10 m. (c) Photograph and (d) sketch of the pit wall at site TW4 (terrace 4). A layer of fine-grained overbank deposits, locally as much as a couple of meters in thickness, exists at the top of most terraces. The length of the yellow bar is 1 m.

Table 1. Measurements of the River Terrace Sediment Thickness Above Straths Along Hsiukuluan Canyon[a]

Site[b]	Terrace Level[c]	Sediment Thickness, m
A	3 (TW)	6.4
B	4 (TW)	6.5
C	4 (TW)	4.1
D	1 (TW)	3.8
E	6 (TW)	7.0
F	6 (TW)	5.5
G	6 (TW)	9.8
H	4 (TW)	0.3
I	6 (TW)	4.0
J	4 (CM)	6.9

[a]Sites of measurement are shown in Figure 4.
[b]See Figure 4.
[c]TW, Tewu loop; CM, Chimei loop.

Central Range. A small portion of the gravels is derived locally from volcanic breccia of the Tuluanshan Formation. The gravels of the higher Tewu terraces are virtually all volcanic, indicating either that a thick tributary alluvial fan overlies the gravels of the main river, or that the small terraces are entirely produced by a tributary originating in the Coastal Range.

[23] Downstream from the Chimei fault, where the river incises the volcanic Tuluanshan Formation, river terraces are much more poorly developed (Figure 4). Only scattered terraces with very thick sediment cover are present. The clasts of these thick cover beds are predominantly very large and angular boulders. Thus these terraces are likely to be eroded remnants of tributary alluvial fans that covered the main channel of the river. If so, they do not provide as adequate a constraint for determining uplift rates as those strath terraces in the western half of the canyon. Fluvial terraces merge with well-developed marine terraces [e.g., *Liew et al.*, 1990] at the easternmost part of Hsiukuluan canyon, near the small village of Takangkou.

3.2. Age of Terraces

[24] None of the river terraces in Hsiukuluan canyon is capped by a lateritic soil. Elsewhere in Taiwan, a lack of lateritic soil indicates that the terraces are less than about
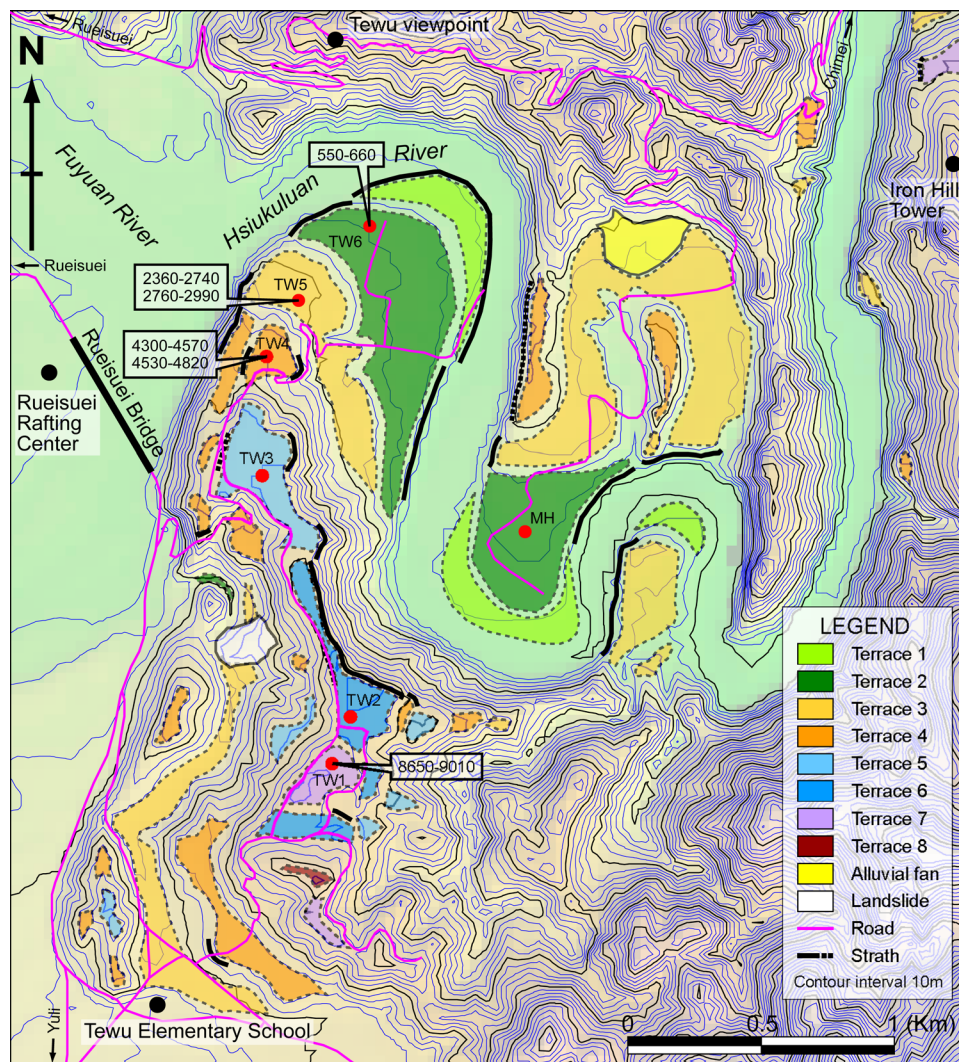

Figure 7a. Detailed map of the fluvial terraces of the Tewu and Monkey Hill loops of western Hsiukuluan canyon, showing sampling sites and the strath contacts. Ages of terraces are calibrated ages (2σ), in calibrated years B.P. (cal B.P.).
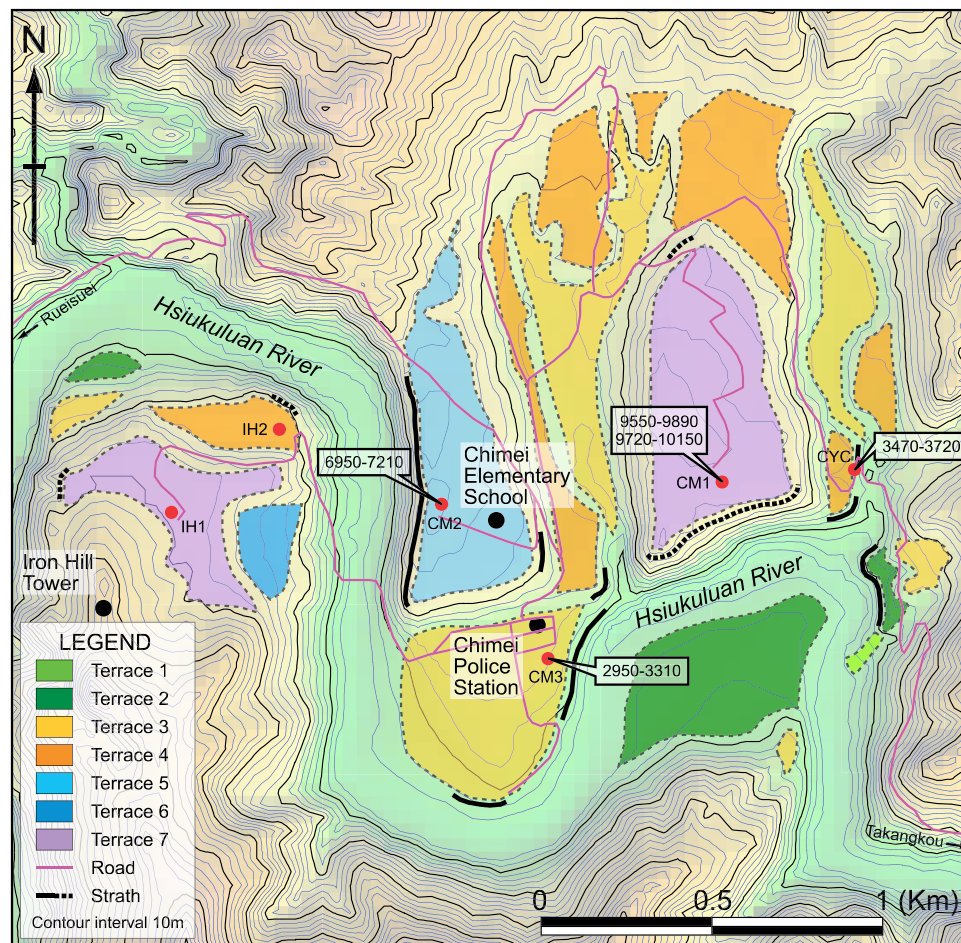
Figure 7b. Same as Figure 7a but map of terraces of the Iron Hill and Chimei loops.

50 kyr old [*Y.-G. Chen*, 1988]. Therefore the Hsiukuluan terraces should be within the range of radiocarbon dating. Since wood samples are scarce in terrace outcrops, we dug small, shallow pits into the terrace surfaces, hoping to expose datable organic material.

[25] In all, we have dug more than a dozen pits, on terraces of all four loops (Figure 7). Several pits yielded charcoal samples. Most of these samples came from terraces that have a thick layer of fine-grained overbank deposits. In the rare cases where we could collect multiple samples from different depths, we were able to constrain the duration of overbank deposition from the ages of these samples.

[26] Figure 8 shows all of the stratigraphic columns constructed from exposures in the walls of the pits. The analytical results for all of the samples we collected are listed in Table 2. Our colleagues at Lawrence Livermore National Laboratory performed all age determinations by accelerator mass spectrometry. The multiple samples from sites CM1 and CM3 show that the fine-grained overbank deposits overlying the gravels have a depositional history that spans more than a couple thousand years. Since Hsiukuluan canyon is very narrow, we suspect that this long history may reflect slack water caused by occasional landslides that obstructed the course of the river and forced it to deposit overbank sediments on terraces high above the active channel. In fact, even without landslide damming, the water level during the most severe typhoons can rise more than 20 m above normal, according to local witnesses. This would explain the unusually young ages we have found at sites such as CM1 and CM3.

[27] Therefore ages obtained from samples below the top of the gravels are generally considered more reliable [e.g., *Lavé and Avouac*, 2000, 2001]. For the same reason, we chose not to use the age obtained from the IH1 site, since it has an unusually young age for such a high terrace. Also, we did not use the ages from the MH site, because one of the samples there indicates a recent age, probably indicating flood deposition during a large typhoon.

[28] The ages we obtained for the terraces along Hsiukuluan canyon show that the higher terraces of the Tewu loop are a little more than 10 kyr old (Table 2). The highest terrace of the Chimei loop (site CM1) has a similar age, but its elevation above the modern riverbed is much lower. The paleochannel of the major meander loop of Chimei was abandoned between 3 and 4 ka.

3.3. Reconstructions of River Patterns in the Past

[29] The ages of terraces obtained from the charcoal samples enable reconstruction of the river course at several times in the Holocene (Figure 9). We have tested the

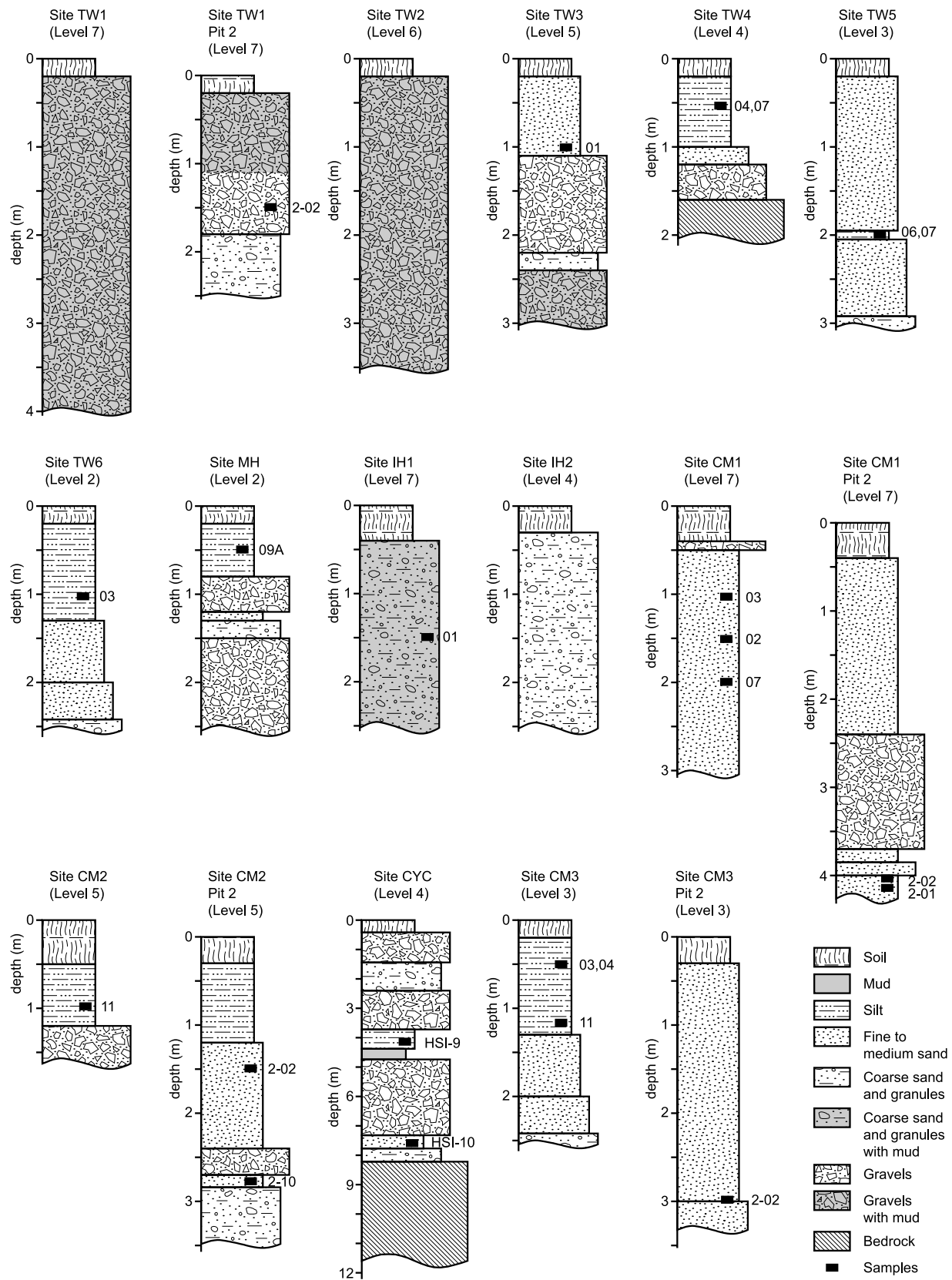**Figure 8.** Stratigraphic columns of all sampling sites. Site CYC is an outcrop of terrace 4 exposed during a road construction. All other sites are sediment pits dug on terraces surfaces in this research. Locations of charcoal samples dated in this research are also shown, with sample numbers next to them. Except for site CYC, where full sample numbers are shown, all other sample numbers are shown without site names.

Table 2. Analytical Results of All of the Samples Dated in This Research

Sample	Site	GPS Location of Site		Terrace Level	Age,[a] years B.P.	Calibrated Age (2σ),[b] cal B.P.	Strath Elevation Above Current Riverbed, m	Incision Rate, mm/yr
		X	Y					
TW1-2-02	TW1	291223	2597094	7	7980 ± 45	8650–9010	>158	>17.5–18.3
TW3-01	TW3	290950	2598159	5	700 ± 40	560–710	~128	[c]
TW4-04	TW4	290989	2598597	4	4135 ± 40	4530–4820	~83	~17.2–18.3
TW4-07	TW4	290989	2598597	4	3985 ± 40	4300–4570	~83	~18.2–19.3
TW5-06	TW5	291110	2598826	3	2495 ± 30	2360–2740	~45	~16.4–19.1
TW5-07	TW5	291110	2598826	3	2765 ± 55	2760–2990	~45	~15.1–16.3
TW6-03	TW6	291369	2599098	2	630 ± 40	550–660	~15	~22.7–27.3
MH-09A	MH	291948	2597949	2	125 ± 30	0–270	~12	[c]
IH1-01	IH1	293750	2599608	7	3720 ± 40	3930–4220	~110	[c]
CM1-02	CM1	295341	2599806	7	3765 ± 30	3990–4240	>102	[c]
CM1-03	CM1	295341	2599806	7	3665 ± 35	3870–4090	>102	[c]
CM1-07	CM1	295341	2599806	7	1570 ± 40	1350–1540	>102	[c]
CM1-2-01	CM1	295341	2599806	7	8720 ± 50	9550–9890	>102	>10.3–10.7
CM1-2-02	CM1	295341	2599806	7	8845 ± 40	9720–10150	>102	>10.0–10.5
CM2-11	CM2	294546	2599635	5	85 ± 30	0–260	~90	[c]
CM2-2-02	CM2	294546	2599635	5	165 ± 30	0–290	~90	[c]
CM2-2-10	CM2	294546	2599635	5	6170 ± 35	6950–7210	~90	~12.3–12.9
HSI-9	CYC	295756	2599722	4	3145 ± 70	3080–3550	43	[c]
HSI-10	CYC	295756	2599722	4	3360 ± 50	3470–3720	43	11.6–12.4
CM3-03	CM3	294857	2599213	3	1015 ± 40	790–1050	~37	[c]
CM3-04	CM3	294857	2599213	3	1055 ± 30	930–1050	~37	[c]
CM3-11	CM3	294857	2599213	3	1625 ± 30	1420–1610	~37	[c]
CM3-2-02	CM3	294857	2599213	3	2945 ± 45	2950–3310	~37	~11.2–12.5

[a]All samples were dated in Lawrence Livermore National Laboratory using AMS, with $\delta^{13}C$ corrected.
[b]Calibrated using the CALIB program [*Stuiver and Reimer*, 1993].
[c]These samples appear to be collected from the overbank deposits and have younger ages than the ages of the terraces. Thus they were not used to calculate the incision rate.

validity of the reconstruction by making longitudinal profiles of the river and calculating the approximate sinuosity of the river course, which is the ratio of the actual length of the river between two points to the shortest distance between the points. The current river course within Hsiukuluan canyon has a sinuosity of approximately 2.5. If most of the variables that control river morphology, such as climate and bedrock type, are essentially invariant, then the sinuosity and slope of the river should also remain nearly constant through time.

[30] According to the reconstructions, the Chimei meander loop was active until about 3.5 ka and was abandoned when the Monkey Hill loop became active. The Monkey Hill loop was abandoned after about 2.5 ka, and the sinuosity of the river stayed relatively constant after that, due to the development of the Tewu loop. Although it seems that the river sinuosity was a little lower in more ancient times, this is more likely to be the result of the lack of constraints on both the Monkey Hill and Chimei loops.

4. Incision and Uplift Rates Along Hsiukuluan Canyon

[31] Since all of the dated Hsiukuluan terraces are strath terraces, their ages and the straths' elevation above the current riverbed allow calculation of the average bedrock incision rate since the abandonment of the terraces. The calculated incision rates (Table 2) are likely to be maximum rates, because the deposition of the fluvial sediments containing the datable samples postdates the formation of the

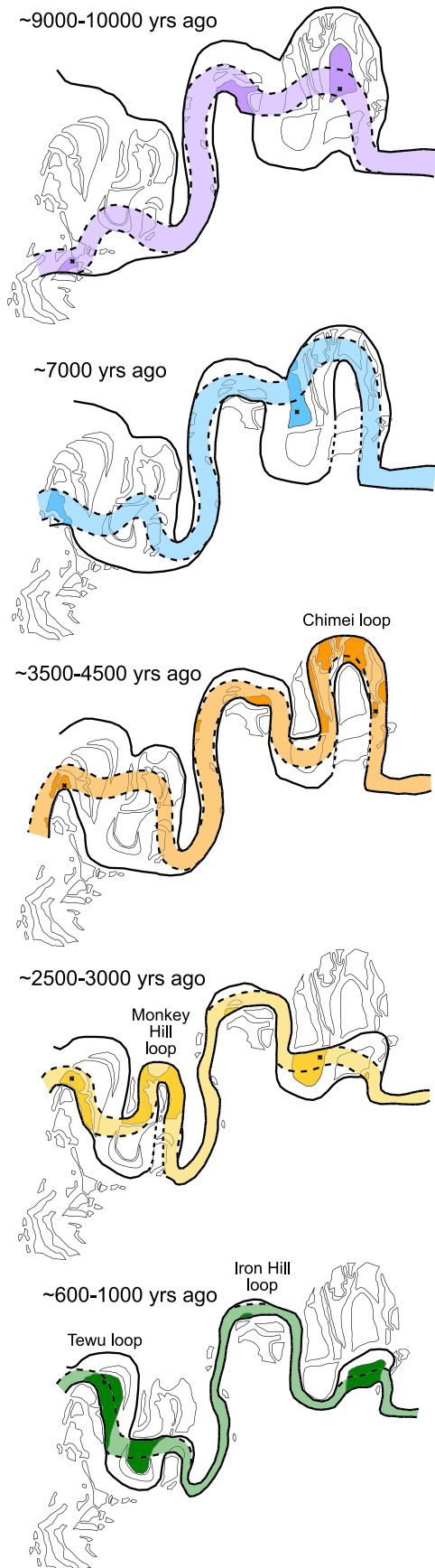strath surfaces. A more detailed discussion of this matter is given by *Lavé and Avouac* [2001].

[32] The cumulative uplift $U(x, t)$ at point x since the formation of the terraces at time t, with respect to the Longitudinal Valley, can be written as [*Lavé and Avouac*, 2000]

$$U(x, t) = I(x, t) + D(x, t) + P(x, t) \qquad (1)$$

where $I(x, t)$ is the incision deduced from the terrace, $D(x, t)$ is the change in local base level, and $P(x, t)$ is the change in elevation at point x due to possible geomorphic contributions of the river, such as changes in river gradient and sinuosity. It has been shown that the geomorphic contribution is dominated by changes in river sinuosity, since the gradient of rivers tend to stay relatively constant (see discussion by *Lavé and Avouac* [2000]).

[33] Therefore the rock uplift rate would be approximately equal to the bedrock incision rate if the following three assumptions are true: (1) There is no change in climate, or the changes did not create significant river pattern change, such as aggradation or incision. (2) There is no significant change in the local river base level, which is the sea level in the case of Hsiukuluan canyon, or the change did not create major changes in accommodation space. (3) The sinuosity of the river stayed relatively constant, so that there is no local aggradation or incision.

[34] Periods of climatic fluctuation have been documented for the Holocene in many parts of Taiwan [e.g., *Kuo and Liew*, 2000]. In fact, many small but locally

Figure 9. Reconstruction of river channels at about 9–10, 7, 3.5–4.5, 2.5–3, and 0.6–1 kyr ago, along the western Hsiukuluan canyon. In each reconstruction the active fluvial channel at that time has the same color as the corresponding river terraces in Figure 7. At any given time, the paleochannels must lie within the confines of the valley sides, defined by the valley walls rising above the corresponding terraces (bold solid lines). Terraces that might have formed along tributary channels do not appear in the reconstructions.

extensive aggradational terraces are present among several small drainages along the eastern slope of the Coastal Range [*Hsieh et al.*, 1994]. These terraces are considered to be the results of three particularly wet periods in eastern Taiwan, about 6, 4, and 1 ka (M.-L. Hsieh, unpublished data, 2005). However, such a record is not present in Hsiukuluan canyon. Not only are there no major aggradational terraces, but also there is no extensive terrace development in any of these periods. We believe that the large drainage area and the long segment of the river upstream from the canyon, in the Longitudinal Valley, damped out any effects of climate change.

[35] The late Quaternary sea level history around Taiwan has been studied intensively [*Chen*, 1993; *Chen and Liu*, 1996, 2000]. According to the ages of emerged corals on the island of Penghu, a stable island in the Taiwan Strait, sea level rose to its highest Holocene level at about 4.7 ka, about 2.4 m above the modern sea level [*Chen and Liu*, 1996]. Subsequently, the sea level has dropped slowly to its current position. Therefore there is no significant sea level change for Hsiukuluan canyon in the past 4.7 kyr. Although there were sea level changes before 4.7 ka, if the slope of the river valley is similar to the slope of the ocean floor right after the river enters the sea, the changes may not create much difference in accommodation space [e.g., *Miall*, 1991; *Schumm*, 1993]. The similarity of the incision rates before and after 4 ka in Hsiukuluan canyon suggests that this may be the case.

[36] Since our paleo-Hsiukuluan reconstructions show that there have been no significant sinuosity changes of the river course, and since there appear to have been no changes in sea level, we are confident that the bedrock incision rates we have obtained for Hsiukuluan canyon are similar to the local rock uplift rates (Table 2). Because the rock uplift of the Coastal Range should be the result of the upthrusting of the Longitudinal Valley fault, we will therefore use these rates to figure out the Holocene rate of dip slip of the fault.

[37] Figure 10 shows the terrace surfaces and straths of all river terraces of the western part of Hsiukuluan canyon, projected onto a plane perpendicular to the general trend of the Longitudinal Valley fault. Upon first inspection, it appears that among the terraces of similar age, those farther upstream are higher above the current riverbed than those farther to the east and closer to the coast. This indicates that the incision rate is higher closer to the Longitudinal Valley fault and decreases to the east. However, because the terraces are not continuous, these ages only provide local incision rates. We attempted to obtain a continuous incision
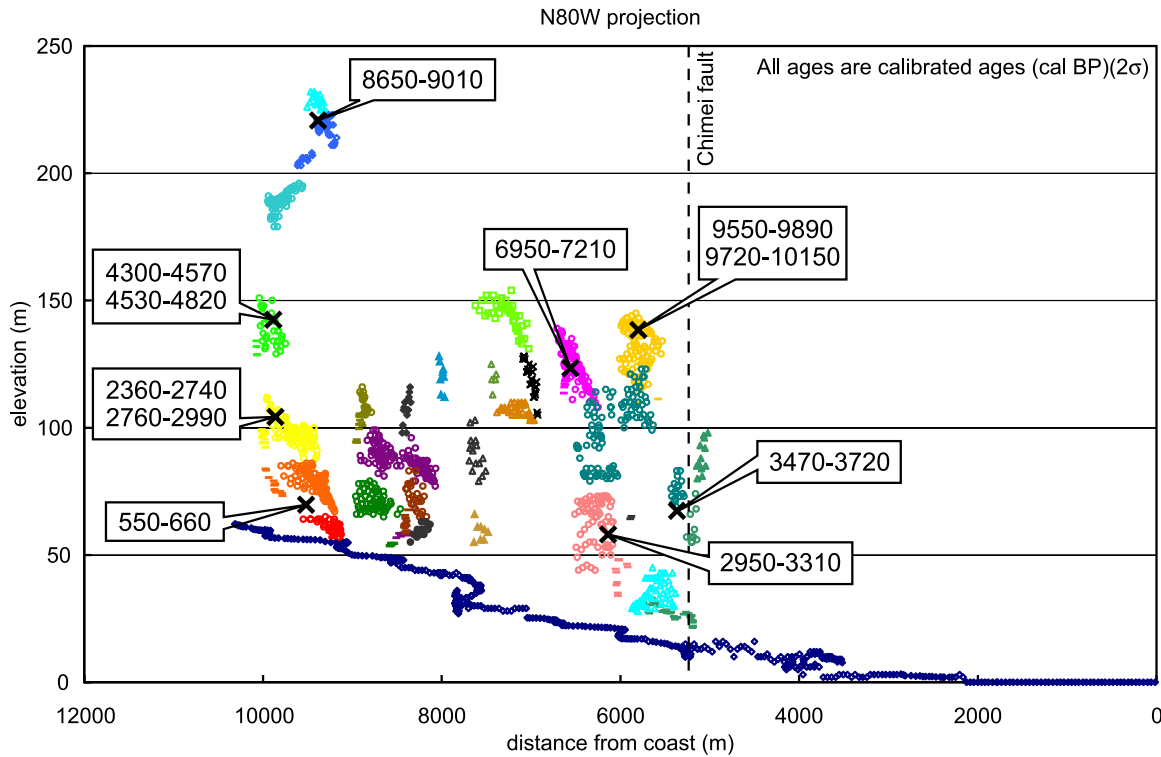
Figure 10. All of the river terraces, together with the sampling sites and the current Hsiukuluan riverbed, projected along N80°W direction. Each color represents a single terrace. Solid dots represent terrace surface measurements from the DEM, and short bars represent terraces straths, measured by laser range finder. All ages are calibrated ages (2σ), in cal B.P.

rate profile along the entire river valley by a method that uses the geometry of the Hsiukuluan River to calculate the river bed shear stress, but it did not yield satisfactory results.

5. Fault-Bend Fold Model

[38] Lacking a continuous incision and uplift rate profile along Hsiukuluan canyon, we moved on to analyze the geometry and dip-slip rate of the Longitudinal Valley fault by assuming that deformation on the hanging wall block of the fault is consistent with a fault-bend fold model. Upon casual inspection, it appears that variations in the pattern of the bedding dip angle mimic the pattern of uplift rate along Hsiukuluan canyon (Figure 4). This is consistent with fault-bend folding [e.g., *Lavé and Avouac*, 2000]. Fault-bend fold models assume that deformation is accommodated by slip along bedding planes, with no change of bed thickness. The geometry of the fault is thus constrained by the bedding dip angles, and the rate of dip slip of the fault can be calculated from the uplift rate and the geometry of the fault. At a given point, the local uplift rate (U), relative to a fixed and rigid footwall, is simply proportional to the sine of the apparent dip angle of the beds at the direction of fault slip (θ′), with this relationship:

$$U = d * \sin\theta' \qquad (2)$$

where *d* is the dip-slip rate along the fault. If the fault eventually turns into a horizontal décollement, *d* will simply

be the horizontal shortening rate perpendicular to the strike of the fault [*Lavé and Avouac*, 2000].

[39] Along Hsiukuluan canyon, θ′ is close to the true dip (θ) of the beds, because most of the bedding attitudes have bedding strike directions similar to the strike direction of the Longitudinal Valley fault (Figure 4). Thus their true dip should be approximately the same as the apparent dip in the direction of fault slip. Nonetheless, several points that are very close to the Chimei fault show anomalous strike directions. Because we have found evidence for drag folding of the beds by the Chimei fault, we decided to discard these dip measurements from our calculations. For the other points, we will use their true dip as θ′.

[40] Since the pattern of bedding dip angle variation is similar to the pattern of the uplift rate, we believe the fault-bend fold model is valid for the Longitudinal Valley fault beneath Hsiukuluan canyon. Continuing on in our analysis, we can fit the variation of the sine of bedding dip angles very well with a polynomial function (Figure 11a). Together with the curve of this polynomial function, we can also plot the uplift rates we obtained from the ages of the terraces along Hsiukuluan canyon using different value of *d* until the two data sets show a good match (Figure 11b). The optimal value of *d* is about 22.7 ± 2.2 mm/yr (see Appendix B for calculation of the uncertainties).

[41] On the basis of the fault-bend fold model, we can also utilize the bedding dip angles of the bedrock to reconstruct the subsurface geometry of the fault (Figure 12). In the model of the fault so constructed, the fault steepens
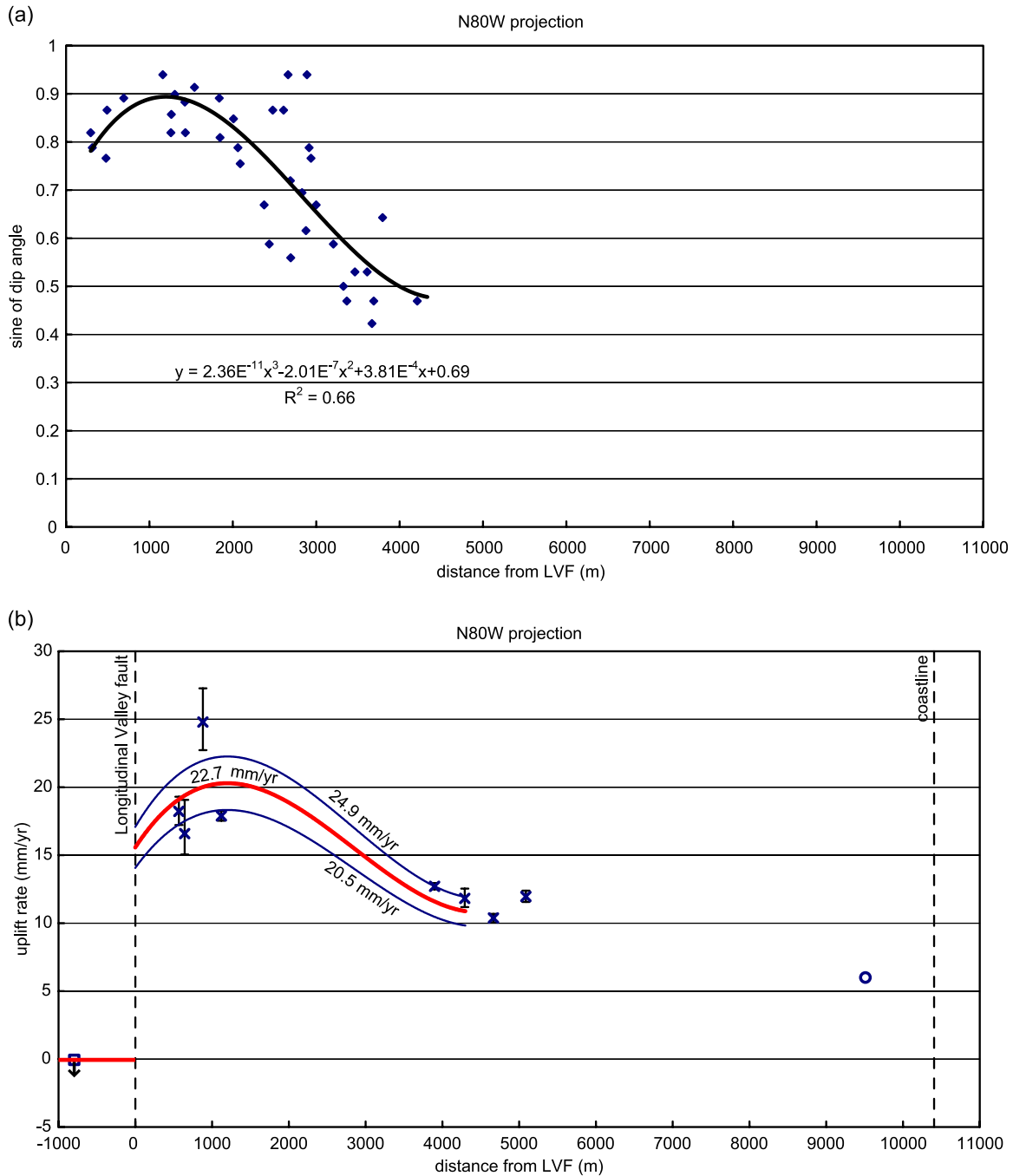
(a)

Figure 11. Fault-bend fold model of the Longitudinal Valley fault along Hsiukuluan canyon. (a) A polynomial function fits very well the variation of the sine of the bedding dip angles of the Paliwan Formation along Hsiukuluan canyon. Bedding dip angle measurements very close to the Chimei fault are not included because they reflect local deformation associated with slip on the Chimei fault. (b) Using different values of dip-slip rate of the Longitudinal Valley fault (d), we can match the polynomial function from Figure 11a with the uplift rates obtained from the river terraces (shown as crosses). The optimal value for d is about 22.7 mm/yr (red line). Taking into account the uncertainty (2.2 mm/yr), d will fall between 20.5 and 24.9 mm/yr (the area between the two blue lines). The circle is the uplift rate obtained from a Hsiukuluan terrace near the river mouth by *Hsieh et al.* [2003]. The square is the minimum subsidence rate of the Longitudinal Valley footwall obtained from site KKL (W.-S. Chen, unpublished data, 2005). See text for discussion.
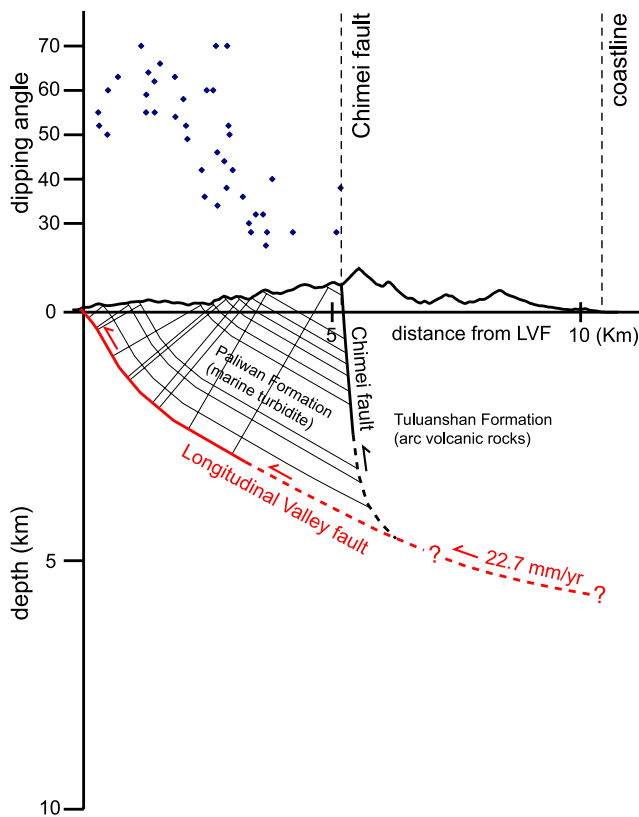
Figure 12. Reconstruction of the subsurface geometry of the Longitudinal Valley fault near Hsiukuluan canyon, from bedrock dip angles. The azimuth of the section is approximately N80°W. This model indicates that the dip-slip rate along the fault is about 22.7 mm/yr and that all of the deformation is accommodated by the slip along the fault plane, with no internal deformation of the beds.

downdip slightly about 1 km below the surface, and then becomes gradually shallower farther downdip. At a depth of about 2.5 km, the fault dips about 30°. If the dip angle continues to greater depth at this angle, the 22.7 mm/yr dip-slip rate yields a horizontal shortening rate of about 19.7 mm/yr in the direction perpendicular to the strike of the fault, which is along the N80°W azimuth. However, the dip of the fault may become shallower at depth, similar to the listric shape of the fault further to the south [*Chen and Rau*, 2002; *Kuochen et al.*, 2004]. Should the fault become horizontal at depth, the horizontal shortening rate along the N80°W azimuth would be equal to the dip-slip rate along the fault, which is 22.7 mm/yr.

6. Discussion

6.1. Shortening Across the Longitudinal Valley Suture

[42] Our analysis of incision and uplift rates across the hanging wall block of the Longitudinal Valley fault at Hsiukuluan canyon has many interesting implications. Our calculation, based on the rock uplift in the hanging wall block of the Longitudinal Valley fault, indicates that the rock uplift corresponds to a shortening rate of no more

than about 24.9 mm/yr along the N80°W azimuth if the footwall block (the floor of the Longitudinal Valley) is fixed. This equals about 27.7 mm/yr in the direction of relative plate motion (306°). This value is smaller than the current shortening rate of about 40 mm/yr along the same direction across eastern Taiwan, shown in Figure 3 [*Hsu et al.*, 2003]. There are several possible explanations for the discrepancy.

[43] First, one could speculate that the decadal rates of shortening revealed by GPS measurements are not equal to millennial shortening rates. Supporting this is a preliminary structural analysis across western Taiwan, which shows that the average shortening rate over the past million years there may be higher than 40 mm/yr [*Simoes and Avouac*, 2006], greater than the rates modeled from the GPS measurements shown in Figure 3. If this is the case, the long-term shortening rates from western and eastern Taiwan will add up to about 70–80 mm/yr. This would be similar to the rates across entire Taiwan from the GPS measurement (Figure 3), although there is still about 10–20 mm/yr of shortening that is not accounted for between easternmost Taiwan and the Philippine Sea plate based upon the plate convergence rate. A structure offshore eastern Taiwan, as proposed by *Malavieille et al.* [2002], might absorb the difference. Although topographic manifestation of such a structure is rather ambiguous [*Shyu et al.*, 2005a], thick sediments offshore eastern Taiwan [e.g., *Schnürle et al.*, 1998] may have obscured deformed topography.

[44] However, if the current decadal rate of shortening is indeed the same as the long-term rate, we need to account for about 12 mm/yr of the total 40 mm/yr across eastern Taiwan that is not accounted for by our estimated slip on the Longitudinal Valley fault. This amount can be provided in at least two ways. For example, slip on the Central Range fault must surely absorb some of the shortening. This amount, however, is not well constrained. The Wuhe Tableland (Figure 2), near Rueisuei, provides a basis for calculating a maximum slip rate along the Central Range fault. The tableland is the result of uplift of the hanging wall block above the fault [*Shyu et al.*, 2002, 2005a, 2006b], and the tableland surface, once the Hsiukuluan River bed, is now at about 170 m above the current river. Wood samples from the river sediments below the tableland surface are older than ^{14}C dating limit of about 50 kyr. Thus the maximum uplift rate of the tableland is about 3.4 mm/yr. Since the dip angle of the Central Range fault is not well constrained, it is difficult to calculate the horizontal shortening across the fault. If, for example, the fault dips 30° westward, a typical dip for a reverse fault, the maximum shortening rate would be about 5.9 mm/yr. Although some unknown reverse faults west of the Central Range fault, within the Central Range, may also accommodate part of the convergence, geomorphic evidence for such structures is not apparent [*Shyu et al.*, 2005a].

[45] Although structures within the Coastal Range, in particular the Chimei fault, may also accommodate part of the plate convergence, our mapping indicates that the fault may not have been active during late Holocene. No geomorphic feature along the fault indicates that the fault is recently active [*Shyu et al.*, 2005a]. Near Chimei, the fault is overlain by fluvial sediments of terrace 3 (Figure 4), which do not show any offset by the fault. The age of the terrace

therefore indicates that the fault has been inactive for at least 3 kyr.

6.2. Subsidence of the Longitudinal Valley Floor

[46] A second explanation for the 12 mm/yr deficit may be that the rate of dip slip of the Longitudinal Valley fault calculated above is not the total dip-slip rate. This is because the fault-bend fold model assumes that the footwall of the fault is fixed, and all deformation is accommodated by the uplift of the hanging wall block. On the basis of the model, the dip-slip rate we estimated is the rate at which the hanging wall block moves along the fault ramp with respect to the fixed footwall and produces the uplift pattern we observed from the river terraces. If, however, the footwall is not fixed and is underthrusting along the fault ramp, the rate we estimated would become only a partial dip-slip rate of the fault. The total rate of dip slip of the fault would be the combination of the overthrust component, which is the value we calculated from the river terraces, and some unknown underthrust component, which would result in the subsidence of the Longitudinal Valley floor.

[47] Similar underthrusting may be occurring along both the Longitudinal Valley and Central Range faults. This would result in higher slip rates on both faults than we estimated above. For example, if both faults dip at 30° at depth, an underthrusting rate of about 6 mm/yr along each fault would increase the dip-slip rates along the Longitudinal Valley and Central Range faults to about 29 and 12 mm/yr, respectively. This would produce about 3 mm/yr of subsidence of the Longitudinal Valley floor and could accommodate an additional 10.4 mm/yr of convergence across eastern Taiwan.

[48] This footwall subsidence, if it exists, could be balanced by sedimentation in the valley, since the major rivers in the valley appear to have sedimentation rates higher than 5 mm/yr [*Hovius et al.*, 2000; *Dadson et al.*, 2003; *Fuller et al.*, 2003]. Some detailed information on the sedimentation rate in the valley and a well-designed leveling profile could test this hypothesis. There is, in fact, a data point at site KKL, a "pressure" ridge along a left-lateral fault, in the valley (Figure 4). There a thick layer of mud, which contains numerous tree trunks older than 50 kyr, is present at a depth of about 3 m (W.-S. Chen, unpublished data, 2005). This yields a subsidence rate of about 0.06 mm/yr (Figure 11b). Since this site is on a pressure ridge and is currently higher than the surrounding valley floor, the subsidence rate of the valley floor must be higher. Further to the south, however, a 3-year-period leveling measurement, tied to tide gauge measurements at the coast southeast of Chihshang, does not show the valley floor to be subsiding [*Liu and Yu*, 1990]. More information is needed to solve this controversy.

[49] In summary, the dip-slip rate along the Longitudinal Valley fault may be higher than what we estimated from the river terraces, since the footwall of the fault may be underthrusting, providing another component of the total dip-slip rate. South of Taiwan, forearc oceanic lithosphere up to 40 km wide is being consumed between the Luzon volcanic arc and the submarine Hengchun Ridge [*Shyu et al.*, 2005b] (Figure 1). In order to create the current geographic pattern, where the Coastal Range is attached to the Central Range, this forearc basement needs to be subducted beneath either the Central Range or the Coastal Range. Although the initial subduction may be in either direction [e.g., *Chemenda et al.*, 1997; *Malavieille et al.*, 2002; *Tang et al.*, 2002; *Shyu et al.*, 2005a], eastward underthrusting is likely to be the major mechanism for the final stage of the forearc oceanic lithosphere removal [*Shyu et al.*, 2005b]. Crustal thickening beneath eastern Taiwan, especially beneath the Coastal Range, has been observed in several seismic investigations [e.g., *Kim et al.*, 2004; *Lin*, 2005; *McIntosh et al.*, 2005]. Such observations are consistent with the hypothesis that the forearc oceanic lithosphere west of the Luzon volcanic arc is still subducting eastward at the latitude of Hsiukuluan canyon, during the final phase of collision.

6.3. Subsurface Geometry of the Longitudinal Valley fault: A Speculative Model for the Evolution of Lithospheric Sutures

[50] Our measurements of bedrock dip angles along Hsiukuluan canyon have enabled us to construct the subsurface geometry of the Longitudinal Valley fault beneath the canyon in the context of the fault-bend fold model. Figure 12 shows that the fault dips steeply initially, and the dip of the fault shallows at about 2.5 km below the surface, to about 30°. This geometry, however, is very different from the geometry of the fault further to the south, near the town of Chihshang, where numerous small earthquake hypocenters define a listric shape with steep dips to much greater depths [*Chen and Rau*, 2002; *Kuochen et al.*, 2004].

[51] It is possible that the Longitudinal Valley fault behaves differently along strike. In fact, although the listric band of seismicity is very obvious around Chihshang, it becomes less apparent both to the north and to the south [*Kuochen et al.*, 2004]. At the latitude of Hsiukuluan canyon, there is a cluster of earthquake hypocenters between 20 and 40 km deep, much deeper than what was suggested by *Kuochen et al.* [2004] to be the Longitudinal Valley fault (Figure 3). There are, on the other hand, several small earthquakes at a shallower depth. Farther to the north, seismicity remains high, but it is very difficult to visualize any clustering of earthquakes that would illuminate a fault plane.

[52] Why does the Longitudinal Valley fault behave so differently along strike? We believe that this is the manifestation of the evolution of the Longitudinal Valley suture, between the Luzon volcanic arc and the Central Range continental sliver. The collision, which began several million years ago, is progressing southward at a rate of about 90 mm/yr [*Suppe*, 1984, 1987]. During the collision, the Luzon volcanic arc and its forearc basins have shortened considerably, to become the current Coastal Range and Longitudinal Valley [e.g., *Chang et al.*, 2001; *Shyu et al.*, 2005b]. The transition area between the Taitung and Hualien domains, near Hsiukuluan canyon, is where this shortening approaches its maximum [*Shyu et al.*, 2005a]. Therefore, at Hsiukuluan canyon, the Longitudinal Valley fault should be close to its final, most mature form, whereas what is happening concurrently offshore, south of the Longitudinal Valley, should reveal what was occurring at Hsiukuluan canyon several million years ago. The along-strike difference of the Longitudinal Valley fault is thus reflecting the ongoing maturation of the suture.

[53] We therefore propose the schematic model for the evolution of the Longitudinal Valley suture shown in Figure 13. Before the collision, the forearc oceanic lithosphere subducts beneath the Central Range continental sliver, as is happening near the southern tip of Taiwan, at about 22°N (Figure 13a). Bathymetric evidence suggests that the major structure there is a west dipping thrust fault at the eastern edge of the forearc basin [Shyu et al., 2005a].

When the two nonoceanic lithospheric blocks start to collide, an east dipping reverse fault appears, along which the forearc oceanic crust begins to subduct eastward (Figure 13b). This would be the first generation of the Longitudinal Valley fault, the geometry of which can be observed now at the southern end of the valley, between about 22°40′N and 22°50′N.
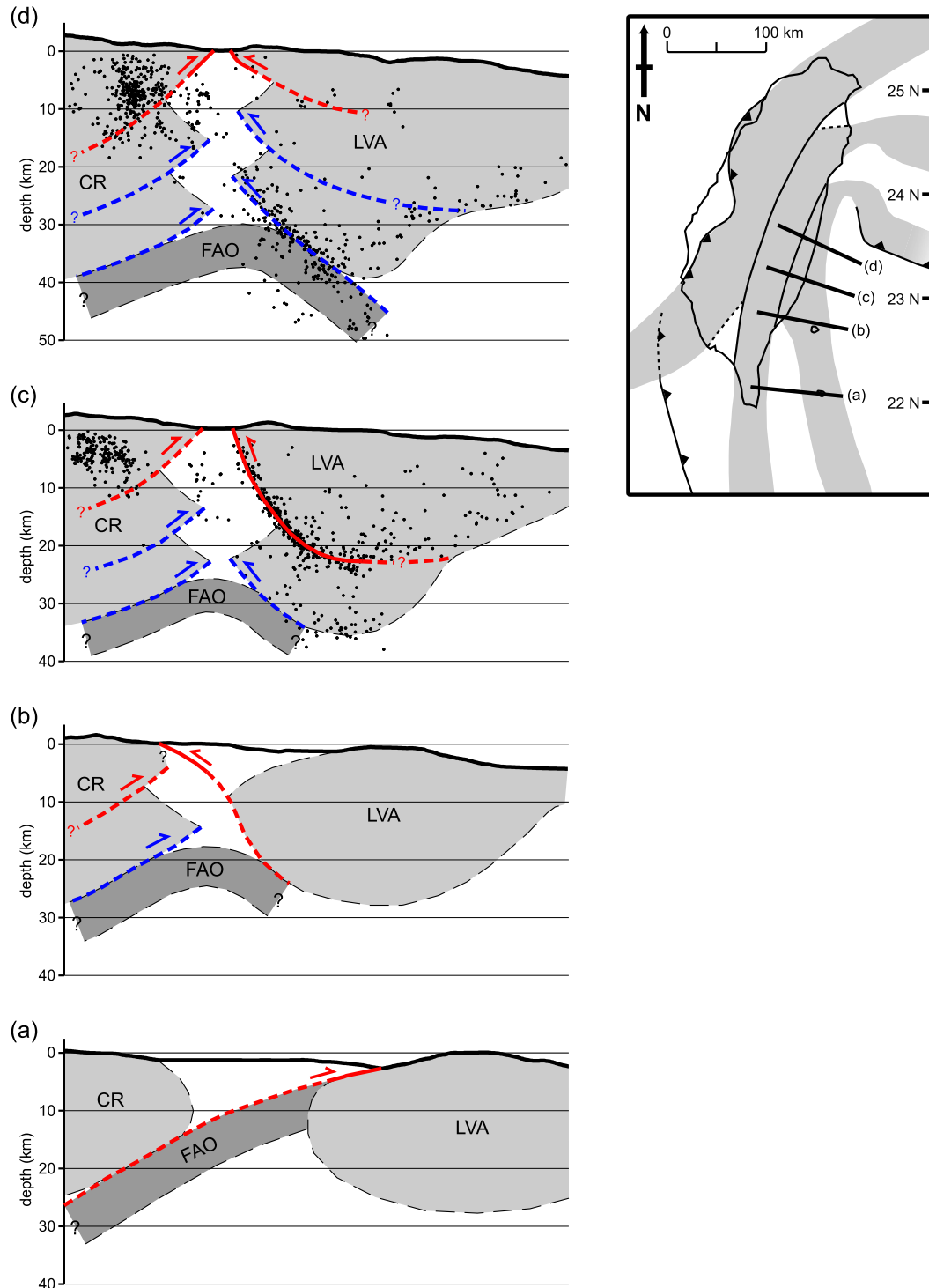

Figure 13

[54] As the two blocks continue to impinge upon each other, thickening of the two blocks next to the suture should occur. We believe this is facilitated by the evolution of multiple reverse fault wedges, with younger ones at shallower depths (Figure 13). This would be an efficient way to thicken the margins of the two crustal blocks as the suture develops. At the latitude of Chihshang, about 23°10′N (Figure 13c), many earthquake hypocenters illuminate the listric-shaped Longitudinal Valley fault, but deeper seismicity appears to indicate an older, deeper reverse fault wedge.

[55] As the suture matures northward (Figure 13d), the shallow Longitudinal Valley fault, reconstructed from the fault-bend fold model for the latitude of Hsiukuluan canyon, about 23°30′N, appears to be the shallowest, youngest generation of the fault. Deeper, there may be several older reverse fault wedges, one of which should connect with the current, listric-shaped fault at the latitude of Chihshang. The deepest seismicity cluster under Hsiukuluan canyon (Figure 13d) may reflect very late stage of subduction of the oceanic forearc crust beneath the Coastal Range.

[56] In all, the evolution of multiple reverse fault wedges facilitates the thickening of the margins of both nonoceanic crust at the suture and creates a "Christmas tree" shape for the Longitudinal Valley suture. Isostatic effect of such crustal thickening may be partly responsible for the very high uplift rates of both the eastern Central Range and the Coastal Range. Between the two nonoceanic blocks of lithosphere, the Longitudinal Valley itself would be a thick pile of sediments, underlain by the subducted forearc oceanic lithosphere. This "Christmas tree" geometry also explains the relatively uniform width of the Longitudinal Valley from south to north, despite the orogeny being much more mature in the north [e.g., *Shyu et al.*, 2005a].

[57] This geometry, however, requires accommodation structures between Chihshang and Hsiukuluan canyon, in order to connect faults at different depth. Geomorphic manifestation of such accommodation structures is scant, but there are, in fact, many other mapped faults present in the bedrock of the Coastal Range. Although the current activity and mechanisms of these structures are not well understood, some of them may be functioning currently as accommodation structures. Further analysis is needed in order to characterize such secondary structures.

[58] We believe that the complex, "Christmas tree" pattern of indentation suggested in Figure 13 might be characteristic of the way suture zones form in general. On the basis of seismic reflection profiles, structures that show indentations at crustal scale have been interpreted for several suture zones, such as the Pyrenees [e.g., *Seguret and Daignieres*, 1986; *Roure et al.*, 1989; *Muñoz*, 1992] and the Urals [e.g., *Juhlin et al.*, 1998; *Steer et al.*, 1998; *Friberg et al.*, 2002]. Nonetheless, these interpretations, which are based on current observations of old, developed sutures, do not provide good insight into their early evolution. In other words, suture zones are nearly vertical structures that have to evolve from the impingement of continental margins, where crust is initially thinner, and little is known about the processes that are responsible for converting the thin continental margin into the thickened crust adjacent to a mature suture. The actively suturing Taiwan orogen may thus provide an insight for the interpretation of old suture zones. In particular, the forearc oceanic crust has been removed and the suture between the Luzon arc and the Central Range continental sliver keeps a near vertical geometry, due to the complex "Christmas tree" indentation pattern.

6.4. Long-Term Uplift Rates of the Coastal Range

[59] The exceptionally high slip rate of the Longitudinal Valley fault also implies that the current fault is a fairly new structure. One of the major questions raised by such a high rate is the different sizes of the two mountain ranges on both sides of the Longitudinal Valley. The Coastal Range, on the hanging wall block of the Longitudinal Valley fault, is much lower than the Central Range, west of the valley. This is odd considering the fault's high rate: If we assume that the erosion rates around the Central and Coastal Ranges are similar, the Longitudinal Valley fault cannot be slipping at such a high rate for very long.

[60] The rocks adjacent to the Longitudinal Valley fault belong to the Paliwan Formation, a Plio-Pleistocene deep marine turbidite unit [e.g., *Chi et al.*, 1981; *Teng et al.*, 1988]. Their original depositional environments are the

Figure 13. Schematic crustal cross sections show our speculative model for the evolution of the Longitudinal Valley suture. Each section is drawn using current topography and observations along the lines specified on the index map. (a) Before suturing, the Luzon forearc oceanic lithosphere (FAO) subducts beneath the Central Range continental sliver (CR). This is currently occurring at about the latitude of the southern tip of Taiwan, at about 22°N. (b) As the Luzon volcanic arc lithosphere (LVA) approaches the Central Range, an east dipping thrust fault appears, allowing the FAO to also subduct underneath the LVA. This is the first Longitudinal Valley fault. Contemporaneously on the west side of the valley, the proximity of the LVA to the CR produces a newer, shallower west dipping thrust fault above the original one. This is the current structural geometry near the southern end of the Longitudinal Valley, between about 22°40′N and 22°50′N. (c) As the suture matures, the two nonoceanic lithospheric blocks both start to thicken by evolving multiple reverse fault wedges, with the younger ones at shallower depth. Here the listric-shaped Longitudinal Valley fault is the second generation of the east dipping fault. This is the current structural geometry at the latitude of Chihshang, about 23°10′N. (d) At the latitude of Hsiukuluan canyon, about 23°30′N, the suture is nearing maturity. The shallower dipping Longitudinal Valley fault, reconstructed using the fault-bend fold model, is the youngest and shallowest of the family of faults dipping under the Coastal Range. In all, the suture has evolved into a "Christmas tree" shape, with a thick pile of sediments between the two nonoceanic lithospheric blocks and underlain by the subducted forearc oceanic lithosphere. Red indicates the youngest and currently active faults at each time frame, and blue indicates older faults that may still be active. Faults are dashed where inferred. Relocated earthquake hypocenters in Figures 13c and 13d were adapted from *Kuochen et al.* [2004]. The earthquakes are from 1991 to 2002 with magnitude larger than 3. Profiles of earthquake hypocenters have a width of 30 km.

forearc and intra-arc basins around the Luzon volcanic arc, at water depths of about 3–4 km [e.g., *Chen and Wang*, 1988; *Teng et al.*, 1988]. Currently, these rocks have a maximum elevation of about 1 km in the Coastal Range. Therefore the million year uplift rate of these rocks since their deposition is only about a couple of mm/yr. Furthermore, since these rocks are not metamorphosed, they have not been buried much deeper than several kilometers. This also yields a long-term exhumation rate much less than 5 mm/yr.

[61] This very low long-term rock uplift rate and the high recent slip rate of the Longitudinal Valley fault implies that the current rapid uplift of the Coastal Range, produced by the slip on the Longitudinal Valley fault, is a rather young phenomenon. At an uplift rate of 20 mm/yr, the uplift may have started only a couple hundred thousand years ago. This implication is consistent with the fact that there is no Longitudinal Valley fault equivalent further south, in the Lutao-Lanyu Domain of the Taiwan orogen [*Shyu et al.*, 2005a] (Figure 13a). In fact, very clear bathymetric evidence suggests that the major structure in the Lutao-Lanyu Domain is a west dipping thrust fault at the eastern edge of the forearc basin [*Shyu et al.*, 2005a], and that the westward underthrusting is the major mechanism for the consumption of the forearc oceanic lithosphere there [*Shyu et al.*, 2005b].

[62] The Longitudinal Valley fault is therefore the product of the final episode of the evolution of Taiwan's eastern suture. This structure appeared when most of the forearc lithosphere had been consumed and the volcanic arc started to impinge upon the Central Range continental sliver [*Shyu et al.*, 2005b] (Figure 13b). At the latitude of Hsiukuluan canyon, this is likely to have begun a couple hundred thousand years ago. After its appearance, this structure absorbed most of the shortening by the deformation of the forearc sediments, and several generations of this structure evolved into a series of reverse fault wedges (Figure 13), creating the "Christmas tree" shape of the Longitudinal Valley suture. Further to the north, where the volcanic arc has fully docked to the continental sliver of the Central Range, the Longitudinal Valley fault has become a predominantly left-lateral fault.

6.5. Earthquake Potential of the Longitudinal Valley Fault

[63] From the ages of the Hsiukuluan River terraces, we have calculated the minimum millennial rate of dip slip of the Longitudinal Valley fault. Using this rate and our limited knowledge of historical earthquakes along the fault, we can start to evaluate preliminary earthquake recurrence intervals of the fault.

[64] The most recent earthquake with surface ruptures occurred on the Longitudinal Valley fault is the earthquake couplet in 1951 [*Shyu et al.*, 2006a] (Figure 2). This earthquake was produced by rupture of two separate sections of the fault, about 45 km in total length but 20 km apart, with a maximum coseismic offset of up to 2.1 m. Average coseismic uplift along the fault is approximately 0.5–1 m. From the river terraces, we know that the long-term uplift rate near the fault is about 20 mm/yr. Therefore, if the 0.5–1 m event in 1951 is a characteristic event on the fault, the average recurrence interval would be merely about 50 years!

[65] It is interesting that the segment of the Longitudinal Valley fault near Hsiukuluan canyon did not rupture during the 1951 earthquakes [*Shyu et al.*, 2006a] (Figure 2). It was the segments both to the north and to the south that ruptured. Therefore this central segment may behave differently, perhaps because it is actually a separate structure, as we have suggested above. Characteristic rupture events with larger coseismic offsets, for example, would result in a longer recurrence interval for this segment.

[66] On the other hand, the long-term shortening may not be absorbed entirely by coseismic deformations. If aseismic creep also releases some component of accumulated strain, longer earthquake recurrence intervals or smaller characteristic events would result. This may be the case for the southern part of the Longitudinal Valley fault near Chihshang, where rapid aseismic creep is well documented [e.g., *Angelier et al.*, 1997; *Lee et al.*, 2001, 2003]. Around Hsiukuluan canyon, however, current data is not adequate to determine if significant aseismic creep occurs [*Yu and Liu*, 1989].

[67] Paleoseismic studies can also help us determine the seismic behavior of the fault. Preliminary paleoseismic works on the segment of the Longitudinal Valley fault north of Hsiukuluan canyon indicate that the fault may have ruptured 2 times before the 1951 event, with intervals of about 160 years (K. P. Fengler et al., Similar slip per event on the Longitudinal Valley fault, eastern Taiwan, manuscript in preparation, 2006). If the fault ruptures at similar intervals near Hsiukuluan canyon, the characteristic rupture of the fault should have coseismic slips greater than 3.5 m. More studies are needed along the central segment of the fault in order to understand better about the strain accumulation and release there.

7. Conclusions

[68] Numerous fluvial terraces, with ages up to 10 kyr, are present along the Hsiukuluan River valley across the Coastal Range in eastern Taiwan. The ages of these terraces provide the basis for calculating the bedrock incision rate, and therefore rock uplift rate along the river valley, in the hanging wall block of the Longitudinal Valley fault. Using this information, we have constructed the subsurface geometry of the fault and calculated its millennial rate of dip slip.

[69] Near Hsiukuluan canyon, the Longitudinal Valley fault likely dips about 50° at its uppermost km or so, but its dip shallows to about 30° by about 2.5 km. Dip-slip rate on the fault is approximately 22.7 ± 2.2 mm/yr, which is also the maximum value of horizontal shortening rate in the direction perpendicular to the strike of the fault.

[70] Our proposed subsurface geometry is very different from what has been suggested further south. This indicates that the fault near Hsiukuluan canyon and further to the south may not be at the same structural depth, a result of the evolution of the Longitudinal Valley suture. Moreover, our calculation suggests that the fault may have been present for only several hundred thousand years, and part of the plate convergence across eastern Taiwan may be absorbed by the underthrusting of the Longitudinal Valley basement. More geodetic, seismic and paleoseismic studies are needed in
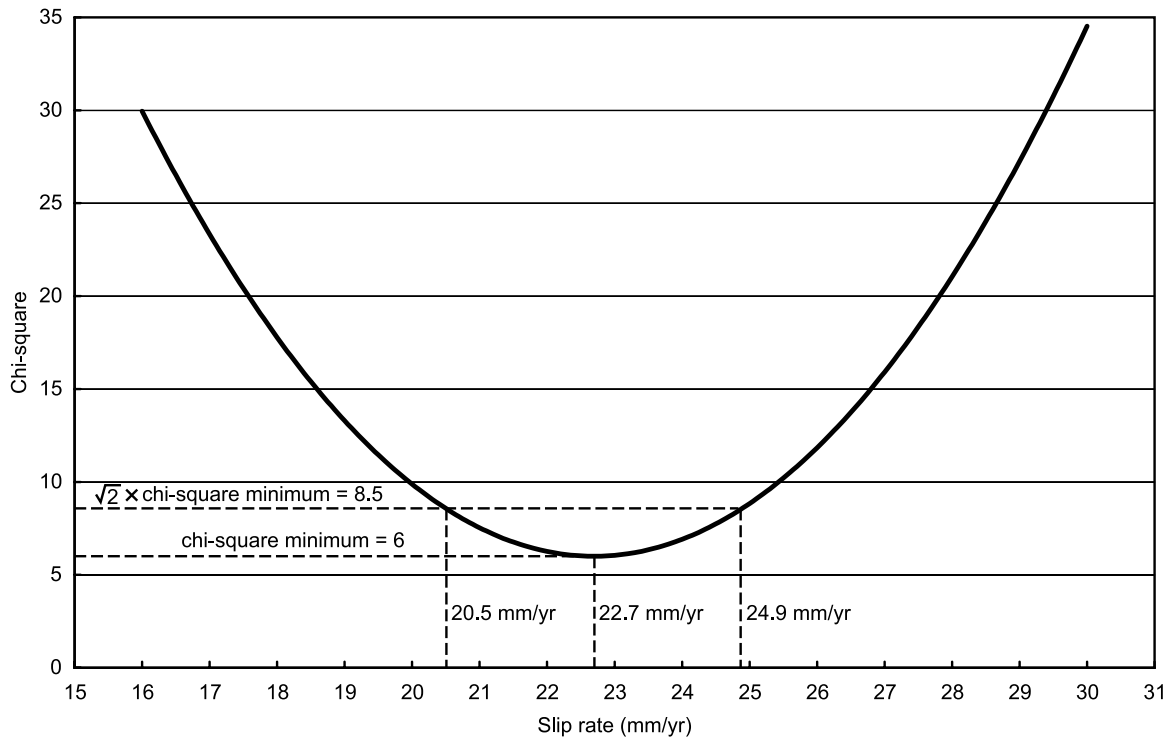
Figure A1. Calculation of the optimum dip-slip rate of the Longitudinal Valley fault and the uncertainty from the fault-bend fold model. The optimum rate corresponds to the minimum value of χ^2. The uncertainty of the rate can be determined by finding the rates that correspond to $\sqrt{2}$ times of the χ^2 minimum, which is about 8.5.

order to test our hypothesis, and to further understand the earthquake potential of the Longitudinal Valley fault.

Appendix A: Determination of Optimal Slip Rate and Uncertainties

[71] Using the polynomial function we obtained from the fault-bend fold model and the uplift rates we obtained from the ages of the terraces along Hsiukuluan canyon, we can determine the optimal dip-slip rate of the Longitudinal Valley fault that fits both data sets. The optimal value of the dip-slip rate is obtained when the calculated χ^2 (chi-square) reaches a minimum. The χ^2 is defined as

$$\chi^2 = \sum [(U_{obs} - U_{mod})/\sigma_i]^2 \qquad (A1)$$

where U_{obs} is the observed uplift rate from the Hsiukuluan terraces, U_{mod} is the uplift rate calculated from the fault-bend fold model, and σ_i is the uncertainty of each observed data point. There are 6 data points that we need to consider (Figure 11b). Therefore, if the uncertainty is well defined, the minimum χ^2 should be about 6.

[72] However, the uncertainties of the data points shown in Figure 11b may not be very well defined. Only the uncertainties resulted from the ^{14}C dating were considered, and we did not consider the uncertainties that may come from the elevation calculation of the terrace straths, simply because of the lack of information due to the limited outcrops. The main uncertainty is due to the irregular geometry of the terrace strath surfaces, which is difficult to evaluate. Thus the uncertainty of each data point may be underestimated, which will result in an overestimation of the χ^2. In order to solve this problem, we decided to calculate the average uncertainty from the minimum value of root-mean-square (RMS), which is defined as

$$RMS = \left[\sum (U_{obs} - U_{mod})^2 \right]^{1/2} \qquad (A2)$$

[73] The minimum value of the RMS appears to be about 2.56 mm/yr. This means that the average uncertainty for each data point of the uplift rates should be about 2.56 mm/yr. Using this value as σ_i for the calculation of equation (A1), we can therefore calculate the χ^2 and use this criterion to determine the uncertainty of the dip-slip rate.

[74] Figure A1 shows the relationship between the calculated χ^2 and different dip-slip rates. The minimum value of χ^2 is then 6, at a rate of about 22.7 mm/yr. This is therefore the optimal dip-slip rate to fit the data sets. The uncertainty of the optimal dip-slip rate can also be calculated by finding the rates that correspond to $\sqrt{2}$ times of the χ^2 minimum, which is about 8.5 (Figure A1). Therefore the optimal dip-slip rate for the Longitudinal Valley fault is about 22.7 ± 2.2 mm/yr. This uncertainty, however, does not take into account the uncertainty in other model parameters than the slip rate, in particular the uncertainty that results from the fault geometry estimations, which is difficult to quantify.

References

Angelier, J., H.-T. Chu, and J.-C. Lee (1997), Shear concentration in a collision zone: Kinematics of the Chihshang Fault as revealed by outcrop-scale quantification of active faulting, Longitudinal Valley, eastern Taiwan, *Tectonophysics*, *274*, 117–143.

Biq, C. (1965), The East Taiwan Rift, *Pet. Geol. Taiwan*, *4*, 93–106.

Bonilla, M. G. (1975), A review of recently active faults in Taiwan, *U.S. Geol. Surv. Open File Rep.*, *75-41*, 58 pp.

Bonilla, M. G. (1977), Summary of Quaternary faulting and elevation changes in Taiwan, *Mem. Geol. Soc. China*, *2*, 43–55.

Bull, W. B. (1990), Stream-terrace genesis: Implications for soil development, *Geomorphology*, *3*, 351–367.

Bull, W. B., and P. L. K. Knuepfer (1987), Adjustments by the Charwell River, New Zealand, to uplift and climatic changes, *Geomorphology*, *1*, 15–32.

Chang, C. P., J. Angelier, C. Y. Huang, and C. S. Liu (2001), Structural evolution and significance of a mélange in a collision belt: The Lichi Mélange and the Taiwan arc-continent collision, *Geol. Mag.*, *138*, 633–651.

Chang, J.-C., T.-T. Shih, S.-M. Shen, and C.-L. Chang (1992), A geomorphological study of river terrace in northern Huatung Longitudinal Valley (in Chinese with English abstract), *Geogr. Res.*, *18*, 1–51.

Chemenda, A. I., R. K. Yang, C.-H. Hsieh, and A. L. Groholsky (1997), Evolutionary model for the Taiwan collision based on physical modelling, *Tectonophysics*, *274*, 253–274.

Chen, H.-H., and R.-J. Rau (2002), Earthquake locations and style of faulting in an active arc-continent plate boundary: The Chihshang fault of eastern Taiwan, *Eos Trans. AGU*, *83*(47), Fall Meet. Suppl., Abstract T61B-1277.

Chen, W.-S. (1988), Tectonic evolution of sedimentary basins in Coastal Range, Taiwan (in Chinese), Ph.D. thesis, 304 pp., Natl. Taiwan Univ., Taipei.

Chen, W.-S., and Y. Wang (1988), Development of deep-sea fan systems in Coastal Range Basin, eastern Taiwan, *Acta Geol. Taiwanica*, *26*, 37–56.

Chen, W.-S., M.-T. Huang, and T.-K. Liu (1991), Neotectonic significance of the Chimei fault in the Coastal Range, eastern Taiwan, *Proc. Geol. Soc. China*, *34*, 43–56.

Chen, Y.-G. (1988), C-14 dating and correlation of river terraces along the lower reach of the Tahan-chi, northern Taiwan (in Chinese), M.S. thesis, 88 pp., Natl. Taiwan Univ., Taipei.

Chen, Y.-G. (1993), Sea-level change and neotectonics in southern part of Taiwan region since late Pleistocene (in Chinese), Ph.D. thesis, 158 pp., Natl. Taiwan Univ., Taipei.

Chen, Y.-G., and T.-K. Liu (1996), Sea level changes in the last several thousand years, Penghu Islands, Taiwan Strait, *Quat. Res.*, *45*, 254–262.

Chen, Y.-G., and T.-K. Liu (2000), Holocene uplift and subsidence along an active tectonic margin southwestern Taiwan, *Quat. Sci. Rev.*, *19*, 923–930.

Chen, Y.-G., W.-S. Chen, J.-C. Lee, Y.-H. Lee, C.-T. Lee, H.-C. Chang, and C.-H. Lo (2001), Surface rupture of 1999 Chi-Chi earthquake yields insights on active tectonics of central Taiwan, *Bull. Seismol. Soc. Am.*, *91*, 977–985.

Cheng, S. N., and Y. T. Yeh (1989), *Catalog of the Earthquakes in Taiwan From 1604 to 1988* (in Chinese), 255 pp., Inst. of Earth Sci., Acad. Sin., Taipei, Taiwan.

Cheng, S.-N., Y. T. Yeh, and M.-S. Yu (1996), The 1951 Taitung earthquake in Taiwan, *J. Geol. Soc. China*, *39*, 267–285.

Chi, W.-R., J. Namson, and J. Suppe (1981), Stratigraphic record of plate interactions in the Coastal Range of eastern Taiwan, *Mem. Geol. Soc. China*, *4*, 155–194.

Dadson, S. J., et al. (2003), Links between erosion, runoff variability and seismicity in the Taiwan orogen, *Nature*, *426*, 648–651.

Friberg, M., C. Juhlin, M. Beckholmen, G. A. Petrov, and A. G. Green (2002), Palaeozoic tectonic evolution of the Middle Urals in the light of the ESRU seismic experiments, *J. Geol. Soc. London*, *159*, 295–306.

Fuller, C. W., S. D. Willett, N. Hovius, and R. Slingerland (2003), Erosion rates for Taiwan mountain basins: New determinations from suspended sediment records and a stochastic model of their temporal variation, *J. Geol.*, *111*, 71–87.

Ho, C. S. (1986), A synthesis of the geologic evolution of Taiwan, *Tectonophysics*, *125*, 1–16.

Ho, C. S. (1988), *An Introduction to the Geology of Taiwan, Explanatory Text of the Geologic Map of Taiwan*, 2nd ed., 192 pp., Cent. Geol. Surv., Minist. of Econ. Affairs, Taipei, Taiwan.

Hovius, N., and C. Stark (2001), Actively meandering bedrock rivers, *Eos Trans. AGU*, *82*(47), Fall Meet. Suppl., Abstract H52B-0389.

Hovius, N., C. P. Stark, H.-T. Chu, and J.-C. Lin (2000), Supply and removal of sediment in a landslide-dominated mountain belt: Central Range, Taiwan, *J. Geol.*, *108*, 73–89.

Hsieh, M.-L., T.-H. Lai, and P.-M. Liew (1994), Holocene climatic river terraces in an active tectonic-uplifting area, middle part of the Coastal Range, eastern Taiwan, *J. Geol. Soc. China*, *37*, 97–114.

Hsieh, M.-L., C. P. Stark, and C.-C. Liu (2003), New radiocarbon dates from the Hsiu-ku-luan River crossing the Coastal Range, eastern Taiwan, and their tectonic implications (in Chinese), paper presented at 2003 Annual Meeting, Geol. Soc. Located in Taipei, Taiwan.

Hsu, M.-T. (1980), *Earthquake Catalogues in Taiwan (from 1644 to 1979)* (in Chinese), 77 pp., Natl. Taiwan Univ., Taipei.

Hsu, T. L. (1962), Recent faulting in the Longitudinal Valley of eastern Taiwan, *Mem. Geol. Soc. China*, *1*, 95–102.

Hsu, Y.-J., M. Simons, S.-B. Yu, L.-C. Kuo, and H.-Y. Chen (2003), A two-dimensional dislocation model for interseismic deformation of the Taiwan mountain belt, *Earth Planet. Sci. Lett.*, *211*, 287–294.

Huang, C.-Y., W.-Y. Wu, C.-P. Chang, S. Tsao, P. B. Yuan, C.-W. Lin, and K.-Y. Xia (1997), Tectonic evolution of accretionary prism in the arc-continent collision terrane of Taiwan, *Tectonophysics*, *281*, 31–51.

Juhlin, C., M. Friberg, H. P. Echtler, T. Hismatulin, A. Rybalka, A. G. Green, and J. Ansorge (1998), Crustal structure of the Middle Urals: Results from the (ESRU) Europrobe seismic reflection profiling in the Urals experiments, *Tectonics*, *17*, 710–725.

Kelson, K. I., K.-H. Kang, W. D. Page, C.-T. Lee, and L. S. Cluff (2001), Representative styles of deformation along the Chelungpu fault from the 1999 Chi-Chi (Taiwan) earthquake: Geomorphic characteristics and responses of man-made structures, *Bull. Seismol. Soc. Am.*, *91*, 930–952.

Kim, K.-H., J.-M. Chiu, H. Kao, Q. Liu, and Y.-H. Yeh (2004), A preliminary study of crustal structure in Taiwan region using receiver function analysis, *Geophys. J. Int.*, *159*, 146–164.

Kuo, C.-M., and P.-M. Liew (2000), Vegetational history and climatic fluctuations based on pollen analysis of the Toushe peat bog, central Taiwan since the Last Glacial Maximum, *J. Geol. Soc. China*, *43*, 379–392.

Kuochen, H., Y.-M. Wu, C.-H. Chang, J.-C. Hu, and W.-S. Chen (2004), Relocation of the eastern Taiwan earthquakes and its tectonic implications, *Terr. Atmos. Oceanic Sci.*, *15*, 647–666.

Lallemand, S., and C.-S. Liu (1998), Geodynamic implications of present-day kinematics in the southern Ryukyus, *J. Geol. Soc. China*, *41*, 551–564.

Lavé, J., and J. P. Avouac (2000), Active folding of fluvial terraces across the Siwaliks Hills, Himalayas of central Nepal, *J. Geophys. Res.*, *105*, 5735–5770.

Lavé, J., and J. P. Avouac (2001), Fluvial incision and tectonic uplift across the Himalayas of central Nepal, *J. Geophys. Res.*, *106*, 26,561–26,591.

Lee, J.-C., J. Angelier, H.-T. Chu, J.-C. Hu, and F.-S. Jeng (2001), Continuous monitoring of an active fault in a plate suture zone: A creepmeter study of the Chihshang Fault, eastern Taiwan, *Tectonophysics*, *333*, 219–240.

Lee, J.-C., J. Angelier, H.-T. Chu, J.-C. Hu, F.-S. Jeng, and R.-J. Rau (2003), Active fault creep variations at Chihshang, Taiwan, revealed by creep meter monitoring, 1998–2001, *J. Geophys. Res.*, *108*(B11), 2528, doi:10.1029/2003JB002394.

Liew, P.-M., and M.-L. Hsieh (2000), Late Holocene (2 ka) sea level, river discharge and climate interrelationship in the Taiwan region, *J. Asian Earth Sci.*, *18*, 499–505.

Liew, P.-M., M.-L. Hsieh, and C.-K. Lai (1990), Tectonic significance of Holocene marine terraces in the Coastal Range, eastern Taiwan, *Tectonophysics*, *183*, 121–127.

Lin, C.-H. (2005), Identification of mantle reflections from a dense linear seismic array: Tectonic implications to the Taiwan orogeny, *Geophys. Res. Lett.*, *32*, L06315, doi:10.1029/2004GL021814.

Liu, C.-C., and S.-B. Yu (1990), Vertical crustal movements in eastern Taiwan and their tectonic implications, *Tectonophysics*, *183*, 111–119.

Malavieille, J., S. E. Lallemand, S. Dominguez, A. Deschamps, C.-Y. Lu, C.-S. Liu, P. Schnürle, and the ACT Scientific Crew (2002), Arc-continent collision in Taiwan: New marine observations and tectonic evolution, *Spec. Pap. Geol. Soc. Am.*, *358*, 187–211.

McIntosh, K., Y. Nakamura, T.-K. Wang, R.-C. Shih, A. Chen, and C.-S. Liu (2005), Crustal-scale seismic profiles across Taiwan and the western Philippine Sea, *Tectonophysics*, *401*, 23–54.

Miall, A. D. (1991), Stratigraphic sequences and their chronostratigraphic correlation, *J. Sediment. Petrol.*, *61*, 497–505.

Muñoz, J. A. (1992), Evolution of a continental collision belt: ECORS-Pyrenees crustal balanced cross-section, in *Thrust Tectonics*, edited by K. R. McClay, pp. 235–246, CRC Press, Boca Raton, Fla.

Roure, F., P. Choukroune, X. Berastegui, J. A. Munoz, A. Villien, P. Matheron, M. Bareyt, M. Seguret, P. Camara, and J. Deramond (1989), ECORS deep seismic data and balanced cross sections: Geometric constraints on the evolution of the Pyrenees, *Tectonics*, *8*, 41–50.

Schnürle, P., C.-S. Liu, S. E. Lallemand, and D. Reed (1998), Structural controls of the Taitung Canyon in the Huatung Basin east of Taiwan, *Terr. Atmos. Oceanic Sci.*, *9*, 453–472.

Schumm, S. A. (1993), River response to baselevel change: Implications for sequence stratigraphy, *J. Geol.*, *101*, 279–294.

Seguret, M., and M. Daignieres (1986), Crustal scale balanced cross-sections of the Pyrenees; discussion, *Tectonophysics*, *129*, 303–318.

Sella, G. F., T. H. Dixon, and A. Mao (2002), REVEL: A model for Recent plate velocities from space geodesy, *J. Geophys. Res.*, *107*(B4), 2081, doi:10.1029/2000JB000033.

Shyu, J. B. H., K. Sieh, L.-H. Chung, Y.-G. Chen, and Y. Wang (2002), The active tectonics of eastern Taiwan—New insights from the two geomorphic tablelands ("the Feet") in the Longitudinal Valley, *Eos Trans. AGU*, *83*(47), Fall Meet. Suppl., Abstract T61B-1278.

Shyu, J. B. H., K. Sieh, Y.-G. Chen, and C.-S. Liu (2005a), Neotectonic architecture of Taiwan and its implications for future large earthquakes, *J. Geophys. Res.*, *110*, B08402, doi:10.1029/2004JB003251.

Shyu, J. B. H., K. Sieh, and Y.-G. Chen (2005b), Tandem suturing and disarticulation of the Taiwan orogen revealed by its neotectonic elements, *Earth Planet. Sci. Lett.*, *233*, 167–177.

Shyu, J. B. H., L.-H. Chung, Y.-G. Chen, J.-C. Lee, and K. Sieh (2006a), Re-evaluation of the surface ruptures of the November 1951 earthquake series in eastern Taiwan, and its neotectonic implications, *J. Asian Earth Sci.*, in press.

Shyu, J. B. H., K. Sieh, Y.-G. Chen, and L.-H. Chung (2006b), Geomorphic analysis of the Central Range fault, the second major active structure of the Longitudinal Valley suture, eastern Taiwan, *Geol. Soc. Am. Bull.*, in press.

Simoes, M., and J.-P. Avouac (2006), Investigating the kinematics of mountain-building in Taiwan from the spatiotemporal evolution of the foreland basin and foothills, *J. Geophys. Res.*, doi:10.1029/2005JB004209, in press.

Steer, D. N., J. H. Knapp, L. D. Brown, H. P. Echtler, D. L. Brown, and R. Berzin (1998), Deep structure of the continental lithosphere in an unextended orogen: An explosive-source seismic reflection profile in the Urals (Urals Seismic Experiment and Integrated Studies (URSEIS 1995)), *Tectonics*, *17*, 143–157.

Stuiver, M., and P. J. Reimer (1993), Extended ^{14}C data base and revised CALIB 3.0 ^{14}C age calibration program, *Radiocarbon*, *35*, 215–230.

Suppe, J. (1984), Kinematics of arc-continent collision, flipping of subduction, and back-arc spreading near Taiwan, *Mem. Geol. Soc. China*, *6*, 21–33.

Suppe, J. (1987), The active Taiwan mountain belt, in *Anatomy of Mountain Chains*, edited by J. P. Schaer and J. Rodgers, pp. 277–293, Princeton Univ. Press, Princeton, N. J.

Tang, J.-C., A. I. Chemenda, J. Chéry, S. Lallemand, and R. Hassani (2002), Compressional subduction regime and initial arc-continent collision: Numerical modeling, *Spec. Pap. Geol. Soc. Am.*, *358*, 177–186.

Teng, L. S. (1980), Lithology and provenance of the Fanshuliao Formation, northern Coastal Range, eastern Taiwan, *Proc. Geol. Soc. China*, *23*, 118–129.

Teng, L. S. (1982), Stratigraphy and sedimentation of the Suilien Conglomerate, northern Coastal Range, eastern Taiwan, *Acta Geol. Taiwan.*, *21*, 201–220.

Teng, L. S. (1987), Stratigraphic records of the late Cenozoic Penglai orogeny of Taiwan, *Acta Geol. Taiwanica*, *25*, 205–224.

Teng, L. S. (1990), Late Cenozoic arc-continent collision in Taiwan, *Tectonophysics*, *183*, 57–76.

Teng, L. S. (1996), Extensional collapse of the northern Taiwan mountain belt, *Geology*, *24*, 949–952.

Teng, L. S., W.-S. Chen, Y. Wang, S.-R. Song, and H.-J. Lo (1988), Toward a comprehensive stratigraphic system of the Coastal Range, eastern Taiwan, *Acta Geol. Taiwanica*, *26*, 19–35.

Yu, S.-B., and C.-C. Liu (1989), Fault creep on the central segment of the Longitudinal Valley fault, eastern Taiwan, *Proc. Geol. Soc. China*, *32*, 209–231.

Yu, S.-B., G.-K. Yu, L.-C. Kuo, and C. Lee (1992), Crustal deformation in the southern Longitudinal Valley area, eastern Taiwan, *J. Geol. Soc. China*, *35*, 219–230.

Yu, S.-B., H.-Y. Chen, and L.-C. Kuo (1997), Velocity field of GPS stations in the Taiwan area, *Tectonophysics*, *274*, 41–59.

Yue, L.-F., J. Suppe, and J.-H. Hung (2005), Structural geology of a classic thrust belt earthquake: The 1999 Chi-Chi earthquake Taiwan (M_w = 7.6), *J. Struct. Geol.*, *27*, 2058–2083.

————————————

J.-P. Avouac, J. B. H. Shyu, and K. Sieh, Tectonics Observatory, Division of Geological and Planetary Sciences, California Institute of Technology, Pasadena, CA 91125, USA. (jbhs@gps.caltech.edu)

W.-S. Chen and Y.-G. Chen, Department of Geosciences, National Taiwan University, Taipei, Taiwan.